

Auditory temporal acuity improves with age in the male mouse auditory thalamus: a role for perineuronal nets?

Authors: Quraishe S¹, Newman TA², Anderson LA³.

Author affiliations:

1: SoBS, B85, IfLS, University of Southampton, Southampton SO17 1BJ, UK

2: CES, Medicine, M55, B85, IfLS, University of Southampton, Southampton SO17 1BJ, UK;

3: UCL Ear Institute, UCL, London, WC1X 8EE UK

ORCID ID:

SQ: 0000-0003-4351-0521

TAN: 0000-0002-3727-9258

LAA: 0000-0003-3300-9530

Abbreviated Title (50 chars): Age-related increases in MGB auditory acuity and PNN

Associate Editor: Lisa Nolan / Eric Prager

3-6 Keywords: Medial-geniculate-body, temporal-processing, click-trains, synchronisation, extracellular-matrix, ageing

Grant Information:

Action on Hearing Loss Pauline Ashley Fellowship awarded to LA (PA14)

USAIS funding to TAN

Corresponding Author:

LAA: UCL Ear Institute, UCL, London WC1X 8EE. Tel: +44 2076798978, lucy.anderson@ucl.ac.uk

Data Availability

The data that support the findings of this study are available from the corresponding author upon reasonable request.

Auditory temporal acuity improves with age in the male mouse auditory thalamus: a role for perineuronal nets?

Abstract

The ability to perceive and interpret environmental sound accurately is conserved across many species and is fundamental for understanding communication via vocalisations. Auditory acuity and temporally-controlled neuronal firing underpin this ability. Deterioration in neuronal firing precision likely contributes to poorer hearing performance, yet the role of neural processing by key nuclei in the central auditory pathways is not fully understood. Here, we record from the auditory thalamus (medial geniculate body, (MGB)) of young and middle-aged, normally-hearing male CBA/Ca mice. We report changes in temporal processing of auditory stimuli, with neurons recorded from ventral and medial MGB subdivisions of older animals more likely to synchronise to rapid temporally varying stimuli. MGB subdivisions also showed increased probability of neuronal firing and shorter response latencies to clicks in older animals. Histological investigation of neuronal extracellular specialisations, perineuronal nets (PNNs) and axonal coats, in the MGB identified greater organisation of PNNs around MGB neurons and the presence of axonal coats within older animals. This supports the observation that neural responses recorded from ventral and medial MGB of older mice were more likely to synchronise to temporally-varying stimuli presented at faster repetition rates than those recorded from young adult animals. These changes are observed in animals with normal hearing thresholds, confirming that neural-processing differs between the MGB sub-divisions and such processing is associated with age-related changes to PNNs. Understanding these age-related changes and how they occur has important implications for the design of effective therapeutic interventions to improve speech intelligibility into later life.

Significance Statement

Difficulty discerning speech in older age is partly attributed to changes in neuronal firing patterns throughout the auditory pathways. The contribution of auditory thalamic (MGB) sub-divisions to these age-related changes is poorly understood and, along with interrogation of other central pathways, is often confounded by altered peripheral function. Contrary to expectations, older animals with normal peripheral thresholds showed improved probability of neuronal firing in the MGB. Increased precision throughout the medial MGB is associated with expression of perineuronal nets around discrete neurons, suggesting the aged brain retains significant capacity for anatomical and electrophysiological plasticity to maximise efficiency into older age.

Introduction

Temporally-varying auditory signals are fundamental components of music and communication sounds, from human speech to animal vocalisations. Normally-hearing humans and animals rely on auditory acuity, associated with precisely controlled neuronal firing. This allows the information contained in temporally varying sounds to be perceived across a wide range of time-scales down to a resolution of a few milliseconds. However, this ability is reported to deteriorate in older age, a change that manifests in poorer hearing performance. Here, we record from the auditory thalamus of young and older adult, normally-hearing mice. We report age-related changes in temporal processing and organisation of extracellular specialisations (perineuronal nets, (PNNs) and axonal coats), associated with age, not advanced hearing loss.

Behavioural studies have suggested that deficits in auditory temporal processing, which are most prevalent for brief stimuli presented at fast repetition rates, underlie age-related problems with

speech perception (Fitzgibbons and Gordon-Salant, 1996; Frisina and Frisina, 1997; Gordon-Salant et al., 2011; Martin and Jerger, 2005). Such suggestions are supported by electrophysiological data, associating communication problems with temporal processing deficits within the auditory brainstem (Casparly et al., 2006, 2005), midbrain (Parthasarathy and Bartlett, 2011; Presacco et al., 2016a, 2016b; Walton et al., 1998) or cortex (Mendelson and Ricketts, 2001; Presacco et al., 2016a, 2016b). These age-related deficits in auditory processing throughout the central auditory pathways have been variously linked to alterations in; inhibitory signalling (Casparly et al., 2008), GABAergic transmission (Burianova et al., 2009; Cisneros-Franco et al., 2018; Pal et al., 2019), cholinergic dysfunction (Sottile et al., 2017), parvalbumin positive (PV+) neurons (Cisneros-Franco et al., 2018; Gray et al., 2014; Pal et al., 2019) and glial cells (Tremblay et al., 2012). However, many studies investigating ageing use old animals or animal-models of accelerated ageing to investigate age-related changes within the auditory system, for example CBA\CaJ mice beyond 80 weeks of age, C57\Bl6 mice (Sergeyenko et al., 2013) or Fisher Brown Norway rats (Cai et al., 2018). Such models are confounded by associated issues arising from concomitant peripheral hearing loss, deficits which likely play an important role in altering the final representation of the auditory scene (Sergeyenko et al., 2013). For example, hearing loss has been shown to alter local inhibitory control across the central auditory pathways (Mossop et al., 2000; Scholl and Wehr, 2008; Wang et al., 2011 [review]). It can also lead to sensory cortical remapping and changes in resource allocation (Merabet and Pascual-Leone, 2010 [review]), while decreased audibility has been shown to be detrimental to listeners' auditory temporal processing (Anderson et al., 2013; Humes and Christopherson, 1991; Humes and Roberts, 1990).

When investigations have controlled for peripheral hearing loss, ageing has been shown to have a differential effect on separate regions of the central auditory pathway. Throughout the central auditory pathways, temporal information within an acoustic signal is directly represented in either i) the temporal firing pattern, where the neural activity is phase-locked to the stimulus or ii) the rate of neural activity, where faster temporal rates are represented by monotonic increases in neural firing rate. Recent ageing studies by Presacco et al. (2019, 2016a, 2016b) investigating midbrain and cortical activity within the same subject have shown that while ageing is associated with a decline in phase-locked activity within the inferior colliculus, cortical responses are augmented in older, normally-hearing adults when compared to their younger, normally-hearing counterparts. These results have been supported by recent animal studies which showed a deleterious effect of ageing at the level of the brainstem but enhanced responses to temporally varying stimuli at the level of the primary auditory cortex (Occelli et al., 2019). Different central mechanisms have been proposed to contribute to these potentially paradoxical observations, including changes in central gain as compensation for degraded auditory input (Chambers et al., 2016b, 2016a), changes in cortical connectivity (Peelle et al., 2010), or altered excitatory and inhibitory balance within the aged cortex (Cisneros-Franco et al., 2018; Hughes et al., 2010; Recanzone, 2018; Stebbings et al., 2016). However, the effect of age-related changes on the medial geniculate body (MGB, the principal region of the auditory thalamus), which is directly connected to both the inferior colliculus and the auditory cortex (see Figure 1), has not been considered. The MGB has previously been proposed to be integral in the transformation of temporally varying stimuli from a temporal code (commonly observed in the midbrain and below) to a rate code (commonly observed in the auditory cortex) (Bartlett and Wang, 2007), suggesting that it has an important role in central auditory processing of temporally varying stimuli. Here, we will establish how ageing affects temporal processing across the MGB and propose three potential outcomes: i) if the MGB is unaffected by ageing then we would expect to see no change between young and older adults, ii) if the MGB is merely acting as a relay or information conduit we would expect that temporal processing within MGB to be degraded in a similar manner to that reported in

the inferior colliculus, or iii) that age-related changes in cortical responses, such as increased central gain, have been inherited from thalamocortical inputs.

The MGB is not a homogeneous entity but is subdivided into three principal regions (ventral, MGv; medial, MGM; dorsal, MGD; Figure 1) which have quite different response properties, reflecting the varied inputs to each subdivision. As such, the MGB subdivisions have been proposed to act as conduits for three separate ascending streams of information (the lemniscal/tonotopic, polysensory and non-lemniscal/non-tonotopic pathways) (Anderson and Linden, 2011; Calford and Aitkin, 1983; Rouiller, 1997; Rouiller and de Ribaupierre, 1985). One particular feature of the MGB is the difference in response latencies and ability to synchronise to temporally varying stimuli across the subdivisions. Responses from medial MGB are typically shorter latency and able to follow faster repetition rates of a temporally varying stimulus compared to ventral or dorsal MGB (Anderson and Linden, 2011; Bartlett and Wang, 2011, 2007; Rouiller et al., 1981). Some medial neurons phase-lock at repetition rates comparable with IC neurons (Anderson et al., 2005; Rouiller et al., 1981) which likely reflects the inputs from the brainstem as well as the midbrain (Anderson et al., 2009, 2006; Schofield et al., 2014). Recording from the auditory thalamus therefore not only provides an insight at an intermediary point between the midbrain and cortex, but sampling responses from each of the three main MGB subdivisions allows us to gain an oversight into the effects of ageing on each of the three major ascending auditory pathways, as shown in Figure 1.

Processing rapidly changing temporal stimuli requires a delicate balance of excitatory and inhibitory inputs. Indeed, changes in the excitatory/inhibitory balance with age are one of the most commonly cited suggestions for age-related changes in temporal processing occurring within the central auditory pathways. Recent studies have proposed a role for PNNs; highly specialised extracellular matrix components which, among other functions, may contribute to the regulation of this inhibitory/excitatory balance (Bozzelli et al., 2018 [review]; Brewton et al., 2016; van 't Spijker and Kwok, 2017 [review]). PNNs are primarily associated with fast-spiking, GABAergic, PV+ interneurons (reviewed in (van 't Spijker and Kwok, 2017)), but are also associated with excitatory neurons in the cortex, amygdala and hippocampus (Matthews et al., 2002; Morikawa et al., 2017; Wegner et al., 2003). Chondroitin-sulphate proteoglycans (CSPGs) are a major component of PNNs. The glycosaminoglycan chains of CSPGs in PNNs can be labelled with the lectin *Wisteria floribunda* agglutinin (WFA). Only 2% of the CSPGs present in the mammalian central nervous system are found within PNNs. The remaining 98% are present in the diffuse central nervous system extracellular matrix, including the presynaptic matrix and structures such as axonal coats. Axonal coats are independent of somatic or proximal dendritic compartments of PNNs and typically occur in groups of 3 to 8 on some presynaptic terminals (Gáti et al., 2010). PNNs have been extensively reported throughout the central auditory pathways in young adults of several species, particularly in brainstem nuclei where they are associated with fast synaptic transmission, high-fidelity and binaural processing of sound signals (Sonntag et al., 2015; Weinrich et al., 2018). Given the ability of some neurons within the MGB to synchronise to temporally varying stimuli presented at high repetition rates, it might be expected that PNNs would be associated with MGB neurons, particularly those in the medial MGB. However, very few studies have assessed PNN expression in the MGB, and those that have, report that PNN expression is largely absent from the MGB (Beebe and Schofield, 2018; Fader et al., 2016; Friauf, 2000; Gáti et al., 2010). Within the auditory system, genetic and pharmacological degradation of PNNs leads to a reduction in sound-evoked firing rates and increased neuronal response thresholds in the brainstem (Balmer, 2016; Blosa et al., 2015). At the level of the auditory cortex, PNN/PV deterioration has also been shown to occur within the ageing auditory cortex (Brewton et al., 2016) and in rodent models of presbycusis (Brewton et al., 2016 [C57Bl6 mouse]; Ouda et al., 2015 [Fisher F344 rat]) which likely leads to reduced excitability and gain (Balmer, 2016), while degradation of the

extracellular matrix and PNNs with hyaluronidase in the auditory cortex of adult Mongolian gerbils enhances reversal learning and discrimination performance, without interfering with established-learned responses (Happel et al., 2014).

Here, we recorded neural responses to temporally varying stimuli from all subdivisions of the MGB from young adult (~3 month old, referred to as “young” throughout) or middle-aged (~ 18 month old, referred to as “older” throughout) CBA\Ca mice prior to determining levels of PNNs/axonal coats throughout the MGB. The CBA mouse strain is commonly used in auditory research due to its robust hearing into old age. The age-range of the mice was selected on the basis that the animals would have matured, but would not have developed age-associated peripheral hearing deficits (Hunter and Willott, 1987; Sergeyenko et al., 2013; Spongr et al., 1997; Willott, 1986). Our objective was to establish whether ageing affected the ability of neurons in the different subdivisions of the MGB to synchronise to temporally varying stimuli, and whether any electrophysiological changes would be reflected in changes in expression of PNNs/axonal coats across the MGB. Our data identify that ageing may reduce the number of neurons able to synchronise to temporally varying stimuli across a wide range of repetition rates. Within the ventral and medial MGB, synchronisation at lower repetition rates is reduced, whilst the remaining “synchronised” neurons are able to phase-lock to higher repetition rates (shorter inter-click intervals) than their younger counterparts. Limits of synchronisation in the dorsal MGB were not significantly different from younger animals. This age-related, subdivision-dependent change in temporal processing was reflected in the expression of PNNs. While there were no significant age-related global changes in levels of WFA-labelled extracellular matrix across the MGB, there was a change in the organisation of the WFA labelled structures. In older animals, WFA expression was associated with a condensed, lattice-like organisation, typical of PNNs as well as axonal coats, particularly in the medial MGB. Such alterations suggest that temporal processing at the level of the auditory thalamus may be modified through age-related changes to PNN structure and localisation. Such restructuring of the extracellular matrix may allow the auditory thalamus to alter central gain, maintain appropriate levels of inhibition and enhance synchronisation with age.

Materials and Methods

Subjects. All procedures were approved under the United Kingdom Animals (Scientific Procedures) Act of 1986. Experiments were conducted in 28 male mice of the CBA\Ca strain (Envigo) terminally anaesthetised with ketamine and medetomidine; 13 young-adult (age range 2.3-3.8 months, average 3.0 months) and 15 aged-adult (age range 16.4-18.3 months, average 17.7 months). Male CBA mice have been reported to show age-related threshold shifts faster than female CBA mice (Guimaraes et al., 2004; Henry, 2004), although changes in the endocochlear potential and age-related cochlear pathologies have been described as being more pronounced in female CBA\Ca mice (Ohlemiller et al., 2010). Male CBA\Ca mice were used in the present study to decrease inter-subject variability due to oestrus related changes, avoid comparisons between pre- and post-menopausal states (Guimaraes et al., 2004) and to enable direct comparisons with previously published data-sets. Mice were housed in pairs or small groups within a noise-controlled environment with free access to food, water and environmental enrichment. Animals were examined daily for signs of stress, fighting with cage-mates or age-related illness. All animals were used for both thalamic and auditory brainstem response (ABR) recordings. Tissue was collected from all animals for post-hoc localisation of auditory thalamic recording sites and alternate sections were processed for PNN immunohistochemistry. All physiological and histological data was collected and analysed blind to the age of the animal.

Surgical procedures and acoustic calibration. Surgical procedures were similar to those described previously (Anderson and Linden, 2011). All auditory stimuli were presented free-field to the left ear

(contralateral to the thalamic recording site), using a speaker (FF1, Tucker-Davis Technologies) positioned at -45° in azimuth relative to the animal and at the same elevation as the left auditory canal. A sound-attenuating ear plug was placed in the right ear. Before the start of each experiment, acoustic stimuli were calibrated near the opening of the animal's left auditory canal; after correction, the sound system frequency response was flat to within ± 2 dB from 2 to 90 kHz.

Auditory thalamic recordings. Recording procedures and auditory stimuli were identical to those described previously (Anderson and Linden, 2016). A craniotomy, approximately 2.5 mm in diameter, centred 2 mm lateral to midline and 3 mm caudal to Bregma, was performed on the right-hand side, enabling vertical access to the right MGB. Extracellular single-unit and multiunit recordings were obtained from all major subdivisions of the right MGB. Linear multichannel electrode arrays comprised of up to 16 parylene-coated tungsten microelectrodes (impedance 1–2 M Ω at 1 kHz, WPI, TM33A20) were custom-made to enable simultaneous recording from multiple MGB subdivisions. Electrode arrays were positioned stereotaxically, with a typical starting position of 1.4 mm lateral to midline and 3 mm caudal to Bregma. Electrode arrays were advanced using a hydraulic probe drive (FHC 50-12-1C) controlled from outside the sound-attenuated booth (FHC Neurocraft MCM/MCU). To ensure consistency in depth measurements across penetrations, the motor controller was zeroed as the tip of the microelectrode touched the cortical surface (as confirmed by visual inspection under a microscope and by an acoustic change in the electrode signal). In all penetrations, the electrode was advanced to 2200 μ m below the cortical surface, then left to stabilize for ~ 10 minutes. Neurons were located using 50 μ s clicks presented at variable intensities. Trigger levels were set manually so that action potentials had to exceed a threshold of at least 2x S.D. of the background noise and pass both the positive and negative threshold within 700 μ s of the first threshold crossing. Single units were isolated off-line by manually clustering spike waveforms in up to three dimensions (e.g., peak amplitude, trough amplitude, peak width) using spike-sorting software (Jan Schnupp's Brainware, Tucker-Davis Technologies). All results reported for analysis of pooled multiunit and single-unit data were also confirmed to be valid for single-unit data alone. Once auditory responses were established, recordings were collected during 100 repetitions of a 50 μ s click presented at 60 dB SPL with at least 500 ms inter-stimulus interval. Further recordings were collected during presentations of click trains, and tone-pips of varying frequency and intensity. Click trains were 500 ms in duration and composed of 60 dB SPL clicks with interclick intervals (ICIs) of 1, 2, 4, 6, 8, 10, 20, 50, 100 and 250 ms; responses to 20 repetitions of each train were recorded. To estimate each neuron's characteristic frequency, three repetitions of tone-pips at variable frequencies and intensities were presented in a sequential manner (2-64 kHz, 10-80 dB SPL, tones were presented every 1/6 octave in 5 dB steps; tones had a 5 ms rise/fall time, 100ms duration and were presented with an inter-stimulus interval of 500 ms). Spontaneous activity was measured by recording 100 epochs of 500 ms duration while the speaker was unplugged.

ABR measurements. Subdermal electrodes were placed at the vertex of the skull (+), over the ipsilateral bulla (-), and over the contralateral bulla (ground). Signals were amplified 20x with a Tucker-Davis Technologies low-impedance headstage (RA4LI), digitized with a 16-bit sigma-delta analog-to-digital converter (Tucker-Davis Technologies RA16SD, hardware bandpass filtering 2.2 Hz to 7.5 kHz), recorded at a 24.414 kHz sampling rate, and then bandpass filtered in software between 100 and 3000 Hz (fifth-order Butterworth filter). Stimuli, presented at a rate of 20/s, were either tone-pips (5 ms total duration with 1.5 ms rise/fall time; frequencies 6, 9, 12, 18, 24 and 30 kHz, 500 repeats per stimulus) or clicks (50 μ s in duration, 1000 repeats per stimulus). Stimulus intensities were presented in 5 dB steps from 5 to 80 dB SPL. As per recent work from our laboratory (e.g. Anderson and Linden, 2016; Bakay et al., 2018), ABR thresholds were defined as the lowest sound level at which at least two of the deflections in the ABR waveform exceeded 2xS.D. of the background signal. Measurements of

wave amplitudes were performed using custom Matlab software: a time window containing the wave of interest was selected by the user, and the software then detected maxima and minima of the ABR traces within that window.

Data analysis. All data analyses were conducted blind to the age of the animal. Results of electrophysiological statistical tests are described as “significant” if $p < 0.01$, and as “trends” where $p > 0.01$ but < 0.05 . All statistical tests were nonparametric and two-tailed unless otherwise specified. Non-parametric statistics were used as default to avoid the need to make assumptions regarding the distribution of our data. Recordings of neuronal responses to 100 presentations of a single click presented with an inter-click interval (ICI) of at least 500 ms were used to determine click-evoked firing rates, first-spike latency, and peak latency. Neurons were considered to be responsive to auditory stimuli if a post-stimulus time histogram (PSTH) compiled from 100 click repetitions using 0.5 ms time bins showed a peak in firing that exceeded $2 \times$ S.D. of the neuron’s spontaneous rate. All neurons which showed a significant response to this single click stimulus were included in this study. The first-spike latency to the click was defined as the median of the times at which the first spikes were elicited in response to the click, across 100 click presentations. Latencies were calculated from the PSTH using 0.5 ms bins; similar results were obtained with 0.1 or 0.2 ms bin-widths. Trains of clicks with different ICIs were used to assess the neuron’s ability to follow temporally varying stimuli. The “minimum ICI for synchronisation” was determined to be the minimum ICI for which the vector strength of the entire click train response was significant as determined using the Rayleigh test of uniformity (Rayleigh values > 13.8 , $p < 0.001$). For the fastest ICIs (1-2 ms), the first 6 ms of the response was excluded from vector-strength calculations to ensure that the onset response was not artificially contributing to synchronisation. Spontaneous firing rate was determined by calculating the average firing rate over the 100 epochs of silence (speaker unplugged).

Histological identification of thalamic recording sites. As in Anderson and Linden (2011), discrete electrolytic lesions (5 μ A for 5–7 s) were created a fixed distance apart (as controlled by a hydraulic microdrive) prior to moving the electrode to a new track to indicate the region of recording within the MGB. Histological reconstruction of all recording sites could then be accomplished using the recorded stereotaxic coordinates and estimated corrections for variations due to histological processing. Procedures for histological processing were as described by Anderson and Linden (2011). Briefly, following an overdose of sodium pentobarbital (Euthatal, i.p.), mice were transcardially perfused with 4% PFA (chilled). Brains were postfixed in 4% PFA for 12 h. Coronal sections through the auditory thalamus were cut using a vibratome. Sections were 40 μ m thick and mounted on glass slides in two series of alternating sections.

Visualisation of recording sites. To clearly visualize MGB subdivisions and electrolytic lesions, one series was stained for the metabolic marker cytochrome oxidase by incubating sections for 3–5 h at 37°C in a solution containing 20 mg of diaminobenzidine hydrochloride in 10 ml of distilled water and 30 mg of cytochrome c with 3 g of sucrose in 30 ml of 0.1 M phosphate buffer titrated to pH 7.4.

Immunohistochemistry for assessment of perineuronal nets, axonal coats and parvalbumin (PV) expression. To visualise histological changes in extracellular matrix structures in the MGB, one series of alternating sections mounted onto glass slides were washed 3 times in PBS-0.05% tween (5 mins) and subjected to antigen retrieval for 30 mins at 80°C in citrate buffer (0.01M, pH6). Slides were cooled to room temperature (RT), washed 3 times in PBS-0.05% tween (5 mins), followed by permeabilisation in 2% TX-triton for 1 hr at RT. Slides were blocked in 5% BSA/5% NGS/0.2% TX-triton/PBS for 1 hr at RT. The blocking solution was replaced with biotinylated wisteria floribunda agglutinin (WFA-DAKO; 1:500), and anti-parvalbumin antibody (rabbit polyclonal DAKO; 1:1000) in 5% BSA/1% NGS/0.1% TX-triton/PBS, overnight at RT. Slides were washed 3 times in PBS-0.05% tween

(5mins) and incubated in Streptavidin-488 and Alexa-Goat anti-Rabbit 555 secondary antibodies (1:1000 in PBS). Slides were washed 3 times in PBS-0.05% tween (5 mins) before incubating in 0.25% Sudan black (70% ethanol-filtered) for 90 mins. Sudan black was used to quench autofluorescence from lipofuscin, a fluorescent pigment which accumulates with age in the cytoplasm of cells in the central nervous system (Kajimura et al., 2016; Schnell et al., 1999). After optimisation, 0.25% Sudan Black was applied to sections to control for autofluorescence in the tissue. Slides were washed 3 times in PBS, twice in dH₂O, coverslipped with glycerol and sealed with nail varnish. Fluorescent images of WFA and PV immunostaining were obtained using a 10x and 20x air objectives on a Zeiss Axioplan 2 microscope. All images were taken using the same parameters and exposure times. Image analysis was conducted using ImageJ (NIH, United states). All images were background subtracted using a rolling ball radius: 50 pixels. Regions of interest (ROI) were drawn around MGB subdivisions and integrated density values measured. The ROI defined regions were confirmed using alternating sections stained with cytochrome oxidase. Statistical analysis of immunohistochemistry was performed in GraphPad Prism 7.0. Data are presented as means \pm S.E.M. and were analysed with the unpaired Student's t-test. A p-value of < 0.01 was considered statistically significant.

Results

Neurons were considered to be responsive to acoustic stimuli if the response to 100 repetitions of a single click stimulus elicited an increase in firing rate that exceeded two-times the standard deviation of the neuron's spontaneous firing rate. Using this measure, 481 ventral MGB (179 young adult, 302 older adult), 220 medial MGB (93 young, 127 older) and 65 dorsal MGB (31 young, 34 older) single neurons and multineuronal clusters were considered to be responsive to acoustic stimuli.

Neural response patterns to temporally varying stimuli alter with age

Neural responses to trains of clicks with different inter-click intervals (ICI) were classified as one of three main types: synchronised, non-synchronised or mixed. All three types were found throughout the MGB of both young and older adult mice although the proportions varied as shown in Figure 2d. Across MGB subdivisions and age groups "Synchronised responses" were the primary response type. This response type consisted of neural firing which was well-entrained to the click train over longer ICIs, but after a particular limiting ICI (which varied for each neuron) further reduction of the ICI led to low, or absent firing rates following the onset, which were no-longer synchronised with the stimulus as determined using the Rayleigh test of uniformity (Rayleigh values >13.8 , $p < 0.001$). An example of a synchronised response is shown in Figure 2a; this medial MGB neuron produced highly-synchronised discharges in response to the click train for ICIs from 4-250 ms as determined by significant measures of vector strength (shown as filled data points in Figure 2ai). Shorter ICIs resulted in a response to the onset which in some cases (as in this example) was accompanied by a low, brief, unsynchronised burst of firing, resulting in a monotonic vector strength response function (Figure 2ai) while firing rate recorded over the duration of the stimulus showed a non-monotonic response as ICIs decreased (Figure 2aaii). This non-monotonic relationship between ICI and firing rate was typical of synchronised medial MGB neurons recorded from older adult animals, however synchronised neurons recorded from ventral and dorsal MGB, and young medial MGB showed no relationship between ICI and firing rate (see Figure 4 for more detailed analysis). Not all neurons which showed neural entrainment to the click train responded in a synchronised manner to all ICIs below their limiting ICI. Neurons showing a combination of response patterns were termed "Mixed responses". These neurons responded preferentially to particular shorter ICI(s) than to longer ICIs, as determined by measures of vector strength. An example of a mixed response from medial MGB is shown in Figure 2b; neural firing to a selected range of ICIs (4-50 ms) was both increased (Figure 2bii) and highly synchronised, but responses to the longest ICIs showed no synchronisation giving rise to a non-monotonic vector

strength response function (Figure 2bi, filled data-points show significant synchronisation). Note, this example also shows a non-monotonic association between ICI and firing rate which was the typical response type across all MGB subdivisions for both young and older adult animals however, monotonic associations between ICI and firing rate did also occur. The ICIs eliciting peak firing rates from the mixed response type showed no association with the ICIs eliciting peak vector strengths (data not shown). Neurons which did not show any sustained synchrony for any of the ICIs tested (i.e. Rayleigh values <13.8) were termed “Non-synchronised responses”. Such neurons showed driven bursts of activity in response to the acoustic stimuli which were independent of ICI as shown by the example from medial MGB in Figure 2c.

As shown in Figure 2d, in young adult mice (blue bars) the distribution of neural response patterns to click trains followed the same trend across all three MGB subdivisions with synchronised responses being the primary response type (MGV 70%, MGM 72%, MGD 74%) while mixed responses made up the smallest category for each subdivision (MGV 7%, MGM 13%, MGD 3%). With age (red bars), the proportion of response types altered across the MGB, an alteration which was trending towards significance in the ventral and medial MGB (MGV: $\chi^2(2, N=481) = 6.79, p=0.034$; MGM: $\chi^2(2, N=220) = 6.52, p= 0.038$). While mixed responses increased in all three subdivisions, the category (Sync. or NonSync.) which showed a corresponding decrease in proportion varied. In the ventral MGB (lemniscal) subdivision the proportion of both synchronised and non-synchronised response types decreased, whereas the medial MGB (polysensory) subdivision showed a decrease in the number of synchronised responses and the dorsal MGB (nonlemniscal) subdivision showed a decrease in the number of non-synchronised responses.

Ageing improves the precision of neural firing

To determine whether the move towards more mixed-type responses reflected a decrease in temporal acuity we examined the limit of synchronisation for each neuron or cluster of neurons showing a synchronised response type. We defined the minimum ICI for significant synchronisation to be the smallest ICI at which locking to the click repetition period was observed (i.e. the smallest ICI for which the response showed statistically significant vector strength; see Methods).

Minimum ICIs for synchronisation were significantly shorter in older, compared to young, mice in the ventral and medial MGB subdivisions (Figure 3a left and middle; Wilcoxon rank-sum test for difference in medians, MGV $p= 3.16 \times 10^{-4}$, MGM $p= 7.05 \times 10^{-11}$), although this was not the case for the neurons in the dorsal MGB (Figure 3a right, MGD $p=0.19$). Similar results were obtained in all cases from Kolmogorov-Smirnov tests for differences in distributions (MGV $p=0.0076$, MGM $p=1.49 \times 10^{-9}$, MGD $p=0.77$). Not only were the limits of minimum synchronisation improved with age in ventral and medial MGB, but the vector strengths recorded from the synchronised neurons across the ventral and medial MGB in older adult animals were increased compared to those recorded from the same subdivisions in the younger group (Figure 3b, a repeated measures analysis of variance (ANOVA) showed a significant effect of group for MGV $p=0.0013$ and MGM $p=2.15 \times 10^{-6}$). This was not the case for neurons recorded from the dorsal MGB (MGD, $p=0.056$).

When plotted against ICI, measures of vector strength recorded from neurons with a mixed response typically showed a band-pass function. To establish whether ageing altered the synchronisation of neural firing of mixed neurons, measures of peak or “preferred” synchronisation were recorded from each neuron with a mixed firing pattern (as indicated by the asterisk in Figure 2bi). Neurons in the medial MGB of older adult animals shifted their preferred ICI for synchronisation to significantly shorter ICIs than their younger counterparts (Figure 3c middle), no differences were observed for

ventral or dorsal MGB (Figure 3c left and right; Wilcoxon rank-sum test: MGM $p=0.0030$, MGV $p=0.84$, MGD $p=0.50$).

Ageing alters auditory thalamic responses indicating improvement in acuity

We next asked the question: is the improvement in neural temporal precision a reflection of improved auditory responses across the auditory thalamus? Measures of firing rate over the duration of the click train as well as response latency and probability of firing to a single click presented with ICI of at least 500 ms were used to determine basic auditory responses across the auditory thalamus.

Interestingly, average firing rates to clicks presented at low repetition rates (ICIs of 250 & 500 ms) showed no age-related differences, regardless of subdivision (Figure 4, Wilcoxon rank sum, $p>0.1$ in all cases). However, age-related changes in firing rate were observed with decreasing ICI, particularly in the medial MGB (middle column of Figure 4, repeated measures ANOVA showed a significant interaction between age and ICI for MGM $p=0.0026$, but not MGV $p=0.57$ or MGD $p=0.04$). To ascertain whether the age-related changes in firing rate might impact upon the improved limits of synchronisation, the mean firing rates were examined depending on the neural response pattern of the neuron (Figure 4b-d). Neurons in ventral MGB showed consistent firing across all ICIs, regardless of age or neural response type. However, in the medial MGB it became apparent that the age-related increase in firing rate with ICI was primarily driven by changes to the average firing rate of the synchronised neural response type (Figure 4b middle), with ICIs between 4-20 ms eliciting an increase of between 19.4-21.2 spikes/sec from older adults. Conversely, neural recordings with a mixed neural response type recorded from the medial MGB of older adults had lower firing rates than the younger medial MGB neurons in this group; although some variation with ICI was observed, this variation was not significant (Wilcoxon rank sum test between largest difference [ICI 1 ms] $p=0.13$, Figure 4b, middle). No consistent ICI related changes in firing rate were observed in the dorsal MGB; the older animals with a synchronised response type did show lower firing rates to ICIs < 250 ms than younger animals (Figure 4a-d right) however this difference was only significant at ICI of 2ms (Wilcoxon rank sum, $p=0.0065$).

Differences in distribution of response latency and probability of firing to a single click were observed in both ventral and medial MGB, with a greater proportion of short-latency (Figure 5a) and highly reliable neural responses (Figure 5b) being recorded from both subdivisions in older animals (Table 1). To confirm whether differences in response latency arose due to age-related differences in frequency tuning, the characteristic frequency (CF, the frequency which evoked spikes at the lowest threshold) was ascertained for all neurons showing a significant response to pure-tone stimuli. There was no difference in CF distribution between young and older adult animals for any subdivision (Figure 5c, and Table 1). In addition to evoked responses, measures of spontaneous rate were made across the MGB subdivisions (Figure 5d). The only age-related difference in response observed in the dorsal MGB was a significant decrease in spontaneous firing rate (SR) compared to younger animals (Table 1), there was no difference in spontaneous firing in the ventral or medial MGB of young and older adult animals.

Changes to the central auditory system occur independent of peripheral changes

To determine whether the age-related changes in auditory thalamic responses simply arose from altered input due to changes at the level of the cochlea or auditory nerve, basic evoked-potential measures of auditory nerve and brainstem responses (auditory brainstem responses, ABR) were recorded in response to clicks and pure-tones. The ABR waveform comprises a series of peaks and troughs occurring within the first 10 ms after stimulus onset. The first of these waves (Wave I) is

considered to represent summed activity of the auditory nerve and therefore enables us to determine the extent to which the function of the peripheral auditory system has been affected by age. There were no statistically significant differences between young adult and older adult animals in ABR thresholds to either click or tonal stimulation (Figure 6a, ABR thresholds to click, 6, 9, 12, 18, 24, 30 kHz, student's t-test $p = 0.17, 0.35, 0.17, 0.67, 0.65, 0.37, 0.97$ respectively). Click-evoked Wave I growth functions do show supra-threshold differences between young and older adult animals (Figure 6b), with older adult animals showing shallower growth of Wave I amplitude with sound intensity compared to young adults, suggesting mild age-related deterioration in cochlear-neural function. However, comparison of click-evoked Wave I amplitudes at each individual animal's threshold showed no difference between young and older adult animals (Figure 6c). Collectively, these results suggest that there was no difference in auditory sensitivity between the young and older adult groups. Potentially click-trains presented at 60 dB SPL may have elicited a weaker peripheral activation in the older adult group, however, this was not borne out by the finding that click-evoked neural firing rates averaged across the auditory thalamic subdivisions were not significantly different between young and older adult animals (mean \pm SEM: young MGB 21.5 ± 1.24 spikes/sec, older MGB 22.6 ± 1.25 spikes/sec; Wilcoxon rank sum test $p=0.24$).

Age-related changes in extracellular matrix organisation and perineuronal net localisation within MGB sub-divisions reflect changes in temporal acuity and synchronisation in the central auditory system.

To determine if the improved temporal acuity and synchronisation observed in older animals occurred alongside histological changes within the MGB, we assessed expression and localisation of PNNs and axonal coats using the lectin WFA, a marker routinely used to identify PNNs. MGB subdivisions were confirmed in adjacent sections stained for cytochrome oxidase, allowing PNN/axonal coat expression to be assessed in histologically-defined MGB subdivisions. WFA-labelling of the extracellular matrix confirmed the presence of PNN positive (PNN+) neurons and axonal coats in the MGB (Figure 7), with labelling predominantly localised to the medial MGB (Figure 7a&d). WFA-labelled extracellular matrix in young animals displayed a diffuse, predominantly unorganised, structure throughout the MGB, representative of the general extracellular matrix throughout the central nervous system (Figure 7a). WFA labelling in older animals was condensed and tightly structured around somatodendritic neuronal compartments, typical of PNNs (Figure 7di). The change in structural organisation of the extracellular matrix into greater numbers of PNNs and axonal coats in older animals was not reflected in an increase in the fluorescent intensity associated with WFA immunolabelling in the MGB subdivisions (Figure 7g-i). The medial MGB showed the most robust PNN staining compared to the ventral and dorsal MGB subdivisions (Figure 7a-f). The number and intensity of PNN+ neurons showed the greatest increase in the medial MGB of older animals. WFA-positive PNNs were not observed in young adult animals in the ventral or dorsal MGB. In older animals, PNNs were observed in the ventral MGB (Figure 7j), however, this was still limited in comparison to the medial MGB. The presence of PNNs in the dorsal MGB was negligible in both young and older animals (Figure 7l). PNNs are known to preferentially, but not exclusively, surround fast-firing GABAergic, PV+ interneurons. Consistent with observations in other auditory nuclei and cortical regions (Sonntag et al., 2015), PNN+ neurons that were also PV+ (Figure 7e.iii) as well as PNN+ neurons that were PV- were observed in the MGB (Figure 7biii). Axonal coats, specialised extracellular matrix structures consisting of an aggrecan-based perisynaptic matrix (Cicanic et al., 2018), were observed in young and older adult animals in all subdivisions of the MGB. However, the medial MGB showed the most robust and consistent labelling of axonal coats in young animals, which increased greatly in older animals, (Figure 7k). A small increase in axonal coats was also observed in the ventral MGB (Figure 7k).

The strength of expression and number of structures labelled by WFA, defining PNNs (cell body/proximal dendrite) and axonal coats (2-5 μ M, round/oval) (Gáti et al., 2010) were assessed. The number of both PNNs and axonal coats increased across the MGB in older animals compared to their younger counterparts. The medial MGB showed the greatest increase in PNNs and axonal coats in older adult animals, while the ventral MGB showed a modest increase in PNNs in older animals. The changes in the dorsal MGB were negligible, with no robust PNN and axonal coats present. This implies subdivision specific roles for PNNs in auditory information processing in the MGB, which arise with age.

Discussion

This study was motivated by the desire to establish whether neurophysiological correlates of age-related temporal processing deficits as described in elderly human listeners could be demonstrated to be independent of accelerated peripheral hearing loss. In particular, recent studies have observed age-related decline of auditory brainstem (Bidelman et al., 2014) or midbrain (Presacco et al., 2019, 2016a, 2016b) responses to temporally or spectrally varying stimuli, while responses to the same stimuli in auditory cortex were increased and exaggerated (Bidelman et al., 2014; Ocelli et al., 2019; Presacco et al., 2019). These potentially paradoxical results could arise from age-related decreases in the level of inhibition in the cochlear nuclei and/or midbrain (Burianova et al., 2009; Caspary et al., 2008, 2006), leading to the increased jitter in spike timings and degraded temporal processing ability. Changes in cortical gain (Bidelman et al., 2014; Chambers et al., 2016a; Kotak et al., 2005), intracortical excitatory/inhibitory balance (Cisneros-Franco et al., 2018; Hughes et al., 2010) or connectivity (Peelle et al., 2010) could act to compensate for the degraded ascending input. However, the input from the brainstem and midbrain must first pass through an intermediate processing step – the auditory thalamus – prior to reaching the auditory cortices, yet the degree of degradation or augmentation with age at the level of the auditory thalamus remained unknown.

The aged auditory thalamus actively transforms temporally varying information

Here, we recorded from all three major subdivisions of the primary auditory region of the auditory thalamus; the ventral, medial and dorsal subdivision of the medial geniculate body (MGB) in response to basic and temporally varying stimuli. Recordings were made from young adult (mean 3.0 months) and older adult (mean 17.7 months) CBA/Ca mice. We demonstrated that “synchronised” neurons recorded from the medial and ventral MGB of older adult animals were significantly more likely to be able to phase-lock to the individual components (clicks) of the temporally varying stimuli and were able to follow faster repetition rates compared to younger animals. This change was most pronounced in the medial MGB where the median limiting ICI decreased from 37 ms in young adults to 9 ms in older adult animals. Even the dorsal MGB, a subdivision typically regarded as being less able to follow temporally varying stimuli presented at faster rates, showed no degradation in synchronisation ability with age.

The age-related, subdivision specific changes in physiological responses (and distribution of PNNs, see below) reported here and in previous studies (Richardson et al., 2013) underlines the importance of acknowledging the presence of subdivisions within this brain area. It also likely reflects both age-related changes occurring within the subdivisions and across the different ascending auditory pathways which encompass the MGB subdivisions. The observed improvements in temporal processing with age are generally at odds with the commonly reported age-related deficits in temporal processing (e.g. Caspary et al., 2006, 2005; Mendelson and Ricketts, 2001; Presacco et al., 2016a, 2016b; Walton et al., 1998). Increased synchronisation with age at low modulation rates has been reported in the dorsal cochlear nucleus (Schattman et al., 2008) and central nucleus of the inferior

colliculus (Herrmann et al., 2017). However in both cases, the improved synchronisation is diminished in older animals (compared to younger controls) at higher modulation rates. Such a reduction was not observed in the present study. Here, increased temporal acuity at lower click rates was apparent in synchronised neurons recorded from the older adult ventral and medial MGB, however, these neurons also synchronised to much shorter ICIs than equivalent neurons recorded from younger animals.

With age, firing in the medial MGB not only increased in temporal acuity but also increased in firing rate over comparable ICIs. This increased evoked firing is unlikely to be the result of increased input at the level of the auditory nerve since ABR Wave I amplitudes to a 60 dB SPL click were decreased in older animals. At the level of the MGB, aged animals show a small but significant decrease in GAD67, the rate limiting metabolic enzyme essential for the production of the inhibitory neurotransmitter GABA, and a loss in tonic inhibition (Richardson et al., 2013). These alterations could result in an increased excitability of neurons, manifesting in the increased firing rates observed in synchronised medial MGB neurons. However, since increased excitability usually leads to decreased timing fidelity, which was not the case in the older medial MGB neurons, it is possible the alterations in temporal acuity and firing rate could arise due to an interaction between general decreases in tonic inhibition and changes in the extracellular matrix at the level of the auditory thalamus (see section below). Alternatively, such changes could arise as a result of alterations in the corticothalamic feedback loops as suggested by the observation that MGB firing rates to degraded stimuli increase over repeated presentations (Kommajosyula et al., 2019). The age-related changes in the medial MGB are of particular interest as the medial MGB is thought to act as a polysensory, integrative centre, combining information across auditory and non-auditory areas (see Rouiller et al. (1997) and Winer (1992) for review). Thalamic afferents from medial MGB terminate throughout the auditory cortical layers, with large diameter axons terminating primarily in layer I of both core and belt auditory cortical fields (Huang and Winer, 2000). This has led to suggestions that projections from the medial MGB could be responsible for synchronising remote activity, or provide a common input to functionally separate cortical areas (Huang and Winer, 2000). It is therefore tempting to speculate that with ageing these fast and temporally precise neural projections may be preferentially preserved, or even enhanced, to facilitate auditory cortical processing and synchronisation despite a potentially degraded auditory signal.

It has previously been suggested that the MGB may function to transform temporal coding patterns into neural rate coding patterns (Bartlett and Wang, 2011, 2007), therefore age-related changes in the firing rate may be particularly important in this region. Here, a clear transition between temporal and rate coding was not observed in either young or older animals, however, the transformation from previously reported age-related decreases in synchronisation at the level of the brainstem and midbrain, to the improved synchronisation observed in the current study, implies that the MGB does not act as a simple relay station. Instead the MGB actively transforms the auditory signal and these transformations likely continue into old age.

The difference in our observations compared to previous studies possibly arises both from differences in our stimulation protocol and our definition of the term “older adult”. Here, we used trains of transient clicks as a measure of temporal processing, rather than amplitude modulated stimuli. This enabled us to avoid changes in the envelope shape (which would naturally co-vary with modulation frequency), preventing potential confounds in establishing differences in age-related temporal processing verses envelope shape information (Heil, 2001; Zheng and Escabí, 2013). Neurons throughout the auditory pathway can encode the shape of transient sounds with remarkable fidelity; therefore, it is possible that this feature is better preserved with age. A second, and key, difference

between this and previous studies is the age of our older group. Here we were deliberately targeting animals prior to advanced age-related changes arising in the peripheral auditory system (see section below).

Perineuronal nets are associated with auditory thalamic neurons

PNNs are condensed extracellular matrix structures that surround neuronal cell bodies and proximal dendrites. In addition to PNNs, some synaptic terminals (pre- and post-) are surrounded by an aggrecan-based matrix termed axonal coats. Our results demonstrate PNN-positive (PNN+) neurons and axonal coats in the auditory thalamus and their preferential localisation in the medial MGB compared to the other MGB subdivisions. Consistent with our observations in this study, Gáti et al. (2010) identified ambiguous expression of axonal coats and an absence of PNNs in the dorsal MGB and low PNN and low/medium axonal coat expression in the ventral MGB of young rats (5 months) (Gáti et al., 2010; the medial MGB was not assessed). Axonal coats have also been shown to increase in the thalamic ventral posteromedial nucleus (VPM) in aged (14-20 months), wild-type mice (Cicanic et al., 2018).

The presence of PNN+ neurons and axonal coats in the MGB, particularly within the medial and ventral MGB of older adult animals, supports the changes in increased synchronisation to faster repetition rates. PNNs are associated with brain areas capable of following fast afferent stimulation with precision (Balmer, 2016; Blosa et al., 2015; Favuzzi et al., 2017). Very few studies have assessed PNN expression in the MGB (Beebe and Schofield, 2018; Fader et al., 2016; Friauf, 2000), with only one study, excluding our own, reporting expression of PNNs in the medial parts of the MGB (Beebe and Schofield, 2018). WFA labelling is the commonest method to detect PNNs, however, WFA staining does not detect all forms/compositions of PNN, and therefore, we may have inadvertently excluded expression of some PNNs/axonal coats in this study. This identifies the need for additional markers and experimental approaches to be considered in order to fully explore PNN distribution (Weinrich et al., 2018). Despite this potential under-representation, we observed differences in the organisation and localisation of WFA+ PNNs within the MGB subdivisions. In young adult animals, the WFA-stained PNNs were less organised around the somatodendritic compartment of neurons, while in older animals the staining was more organised, forming condensed net-like structures, typical of PNNs, around many neurons, particularly in the medial MGB. Axonal coats were also more clearly organized (shape and size) and intensely stained in older animals, particularly in the medial MGB. Although the presence of PNNs and axonal coats increased in older animals, this was not associated with an overall increase in WFA-stained extracellular matrix. Such a transition of the WFA-positive extracellular matrix, to a more organised and condensed PNN and AC formation in specific subdivisions of the MGB may arise as a compensatory measure, enabling the MGB to alter the gain and fine-tune the amount of GABAergic neurotransmission, network activity and output to the auditory cortex. This may compensate for the decreased activity and synchronisation of inputs arising from the midbrain and brainstem (Chambers et al., 2016b). The age-related changes in PNNs, particularly in the medial MGB and also the ventral MGB, support our interpretation of the functional data that the MGB does not act as a simple relay between the IC and cortex. Interestingly, although age-related reduction in PNN+ neurons have previously been reported in the auditory cortex of old (14-24 months) CBA/CaJ mice (Brewton et al., 2016), this observation does not hold true for all cortical areas or layers (Ueno et al., 2019). This suggests PNNs are important for region and subdivision-specific plasticity. Indeed, regional differences in PNN distribution and function are also reported within the hippocampus (Carstens and Dudek, 2019). Disruption of PNNs in different brain regions leads to distinct effects. In the perirhinal and visual cortex, removal of PNNs with the extracellular matrix degrading enzyme

chondroitinase enhanced long-term depression (Romberg et al., 2013), but impaired long-term potentiation and depression in the hippocampus (Bukalo et al., 2001).

In subsequent studies it will be important to understand the implications of the age-related changes we observed at the level of the MGB, and how they may alter/maintain cortical function or activity in the same animals. Transgenic mice deficient in PNNs, specifically mice lacking link proteins (Cicanic et al., 2018; Edamatsu et al., 2018), tenascin-R (Bukalo et al., 2007), or aggrecan (Rowlands et al., 2018) could be assessed. These animals have attenuated PNNs but no change in the overall content of CSPG. Additionally, extracellular matrix degrading enzymes, such as ChABC, should be considered for future studies with the caveat that ChABC digestion removes the CS-GAG chains of CSPGs both within PNNs and in the diffuse, general extracellular matrix, both of which have differing effects (Bukalo et al., 2001; Edamatsu et al., 2018; Hirono et al., 2018). Only 2% of CSPGs are found in PNNs, thus ChABC treatment may not be sufficient to elucidate a specific role of PNNs. Therefore both genetic and enzymatic manipulations would be required to understand which component of the extracellular matrix contributes to the age-related changes in the MGB. Understanding the particular trigger(s) which cause the PNN to change expression and organisation with age may be key to preserving auditory temporal processing throughout the life-course. PNN formation is known to occur during critical periods of activity-dependent neuronal plasticity (Myers et al., 2012) and coincides with the development of the fast-spiking properties of the neurons they surround. However, the role lifestyle factors play in the continued (re)organisation of PNN within the auditory pathway is currently unknown. Modulation of PNN expression by sensory manipulations and conditioning has been shown to be important for acquisition of auditory fear memory (learning and consolidation) in response to pure tones in the adult auditory cortex (Banerjee et al., 2017). The auditory pathway may prove to be an ideal space in which to investigate the factors and consequences of remodelling the PNN, leading to greater understanding of the role of PNNs within the various auditory nuclei and suggesting potential targets for future therapeutic intervention.

Age-related changes occur independently of advanced peripheral hearing-loss

It is important to note that much of the previous literature uses aged subjects or models of hearing-loss to focus on the changes in the central auditory system that occur concomitantly with changes arising within the peripheral auditory system (Cai et al., 2018; Sergeyenko et al., 2013). By using young adult (11-15 weeks) and older adult CBA/Ca mice between the ages of 66-73 weeks we aimed to investigate the effects of maturity and ageing on the central auditory system, prior to the accelerated degradation of input arising from age-related changes to the peripheral auditory system. CBA/Ca mice within this age-range have been shown to have minimal (<20%) loss of spiral ganglion cells, inner-hair cells and outer hair cells. However, beyond 80 weeks of age, outer-hair cell loss and auditory threshold deterioration accelerates (Sergeyenko et al., 2013) along with changes in the endocochlear potential, and a loss of strial marginal cells (Ohlemiller et al., 2010). Audiograms plotted from ABR thresholds showed no significant changes with age, although there was an age-related decrease in amplitude of the ABR Wave I at supra-threshold levels which can reflect a degeneration of primary cochlear afferents. Firing rates averaged across the auditory thalamus of older adult animals to clicks presented at the same ICI as for the click ABR were no different to those recorded in younger animals, even within individuals with particularly shallow Wave I growth functions. Therefore, our data may reflect central auditory processing in a fully mature murine system. The age-related changes observed indicate that with ageing the brain retains significant capacity for anatomical and electrophysiological plasticity, with PNN localising with MGB neurons to maximise their efficiency, despite a potential degradation of signal to the central auditory system. One of the limitations of the current study is that it is performed in rodents, however, age-related improvements in auditory processing at the higher

levels of the auditory pathway appear to be conserved across the mammalian species. This is supported by evidence from Presacco et al. (2019, 2016a, 2016b) in humans, where older adults showed substantial degradation of the midbrain response and an exaggeration of the cortical response in both quiet and noise, when compared to younger listeners. Comparisons between normally-hearing and hearing-impaired older adults did not show significant differences in either their midbrain or cortical responses, suggesting that age-related temporal deficits exist independently of those predicted by peripheral hearing loss (Presacco et al., 2019).

Even in the absence of hearing and cognitive impairment, processing temporally varying stimuli such as human speech can be a formidable challenge for elderly individuals. Recent evidence is challenging the traditional view that speech intelligibility decreases simply due to impoverished sensory input and highlights the important contribution of ageing and other lifestyle factors on auditory temporal processing. Understanding how such factors interact has important implications for the design of effective therapeutic interventions to improve speech intelligibility into later life.

Conflict of interest statement

The authors have no conflict of interest to declare.

Table legend

Table 1: Table showing mean \pm S.E.M first spike latency, probability of firing, characteristic frequency and spontaneous firing rate across ventral, medial and dorsal MGB of young (~3m) and older (~18m) adult mice. P-values calculated using Wilcoxon rank sum test and considered significant at $p < 0.01$.

Figures and legends

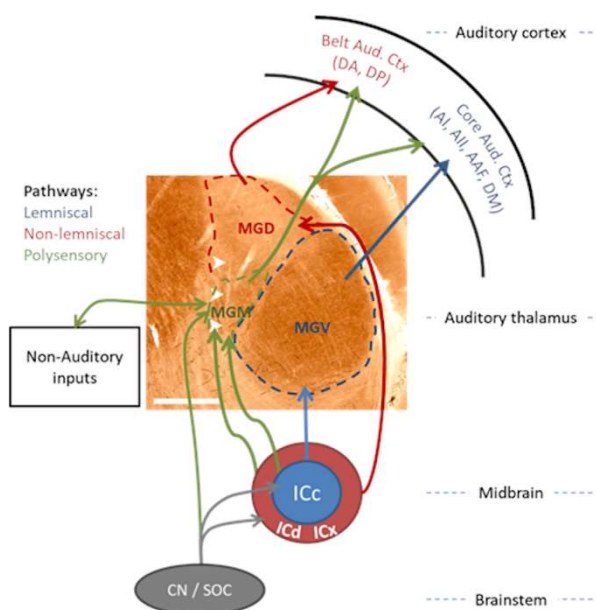


Figure 1: Three ascending pathways run through the auditory thalamus (MGB) to the auditory cortex. A section through the MGB stained for cytochrome oxidase reveals the borders of the three main subdivisions; the ventral (MGV), medial (MGM) and dorsal (MGD). Schematic shows main connections to/from the different MGB subdivisions in the mammalian system which form three main ascending information streams from the midbrain to the auditory cortices: lemniscal (blue), non-lemniscal (red), and polysensory (green) (Anderson et al., 2006; Anderson and Linden, 2011; Rouiller, 1997; Rouiller and de Ribaupierre, 1985). Scale bar on histology image = 1mm. Abbreviations: cochlear nuclei, CN; superior olivary complex, SOC; central, dorsal or external nucleus of the inferior colliculus, ICc, ICd, ICx respectively; primary auditory cortex, AI; secondary auditory cortex, AII; anterior auditory field, AAF; dorso-medial cortex, DM; dorso-anterior cortex, DA; dorso-posterior cortex, DP.

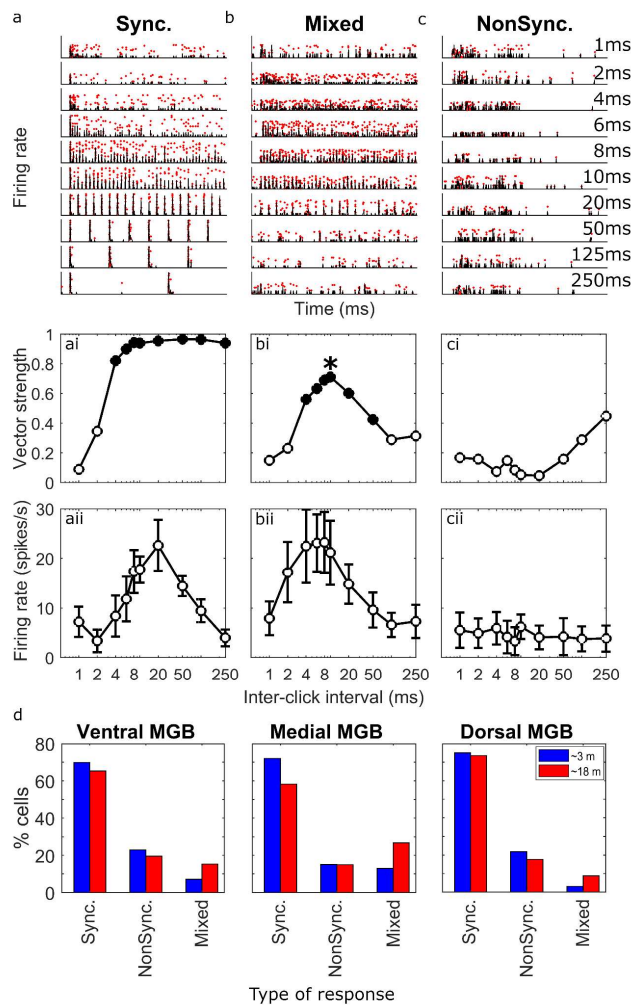


Figure 2: Ageing alters the temporal response patterns to temporally varying stimuli. A-c, raster plots with overlaid peri-stimulus time histogram (PSTH) from example MGM neurons showing a synchronised (a), mixed (b) or non-synchronised (c) response to click-trains of different inter-click intervals (ICI). Ai-ci, plots of vector strength against ICI for the neurons in a-c. Synchronisation of firing to each click train was quantified with the Rayleigh score of vector strength, significant synchronisation is indicated by filled data points. Asterisk in Bi indicates the peak or “preferred” ICI for this mixed response type neuron. Aii-cii, plots of firing rate recorded over the duration of the stimulus against ICI for the neurons in a-c. D, Bar charts showing percentage distribution of each of the response types across the ventral, medial and dorsal subdivisions of the auditory thalamus in young adult (~3m, blue bars) and older adult (~18m, red bars) animals.

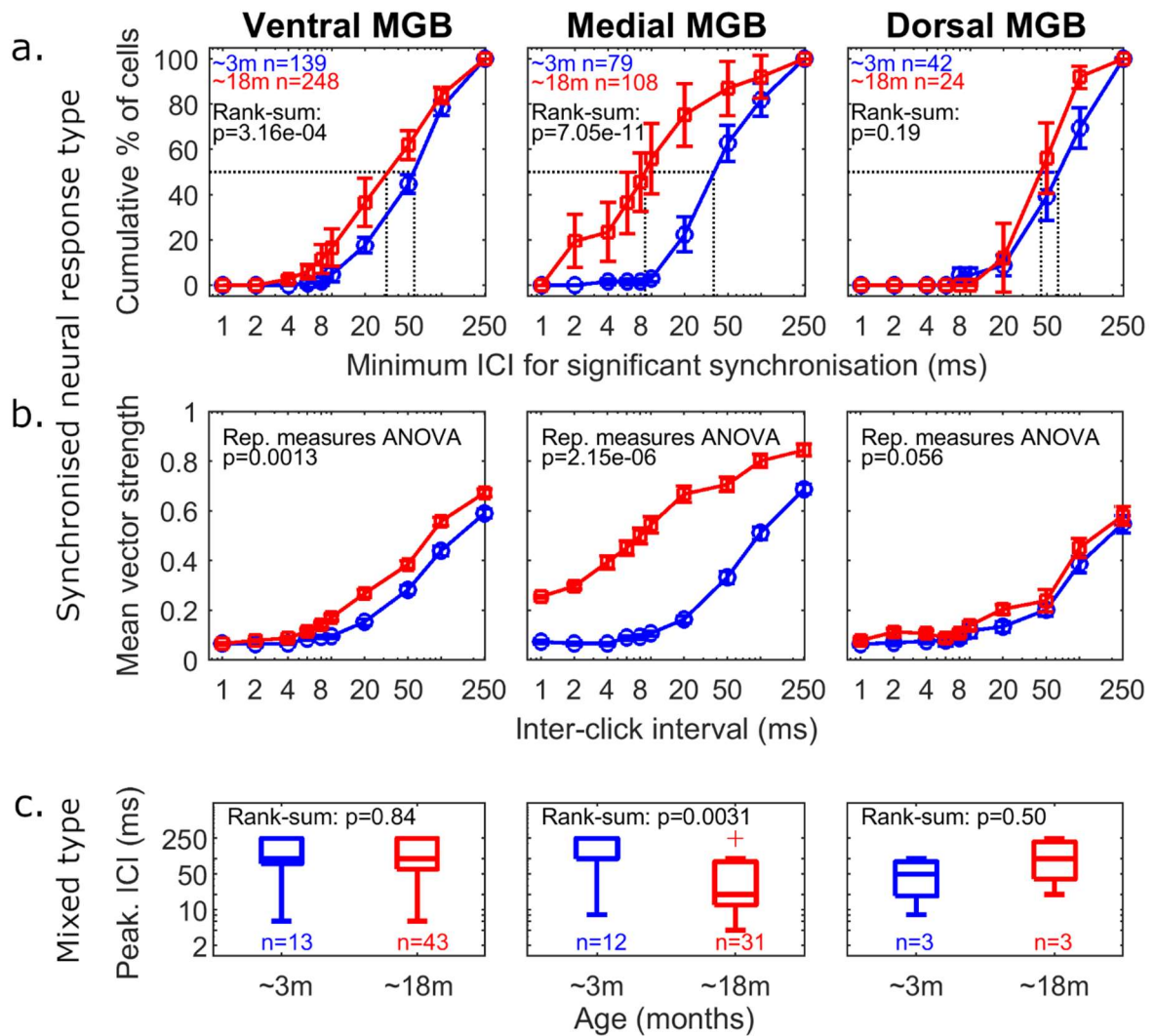


Figure 3: Ageing improves the minimum ICI of synchronised neurons in ventral and medial MGB. A, minimum ICI for significant synchronisation is significantly lower in MGV (left plot) and MGM (middle plot) of older adult animals. No difference in minimum ICI was observed between young and older adult animals in MGD (right column). Results of Wilcoxon rank-sum tests for medians are shown on each plot. Solid red and blue lines with error bars indicate mean \pm S.E.M. for older and young adult animals respectively; dotted grey lines indicate median values. B, mean vector strength of the synchronised response type, recorded across the MGV (left plot) and MGM (middle plot), was higher in older adult animals. C, ICI which elicits the highest vector strength from neurons showing mixed response type to click trains significantly decreases in older MGM (middle) but not MGV (left) or MGD (right). Median values indicated by the central mark and 25-75% percentiles indicated by edge of box, whiskers extend to most extreme data points not considered to be outliers. Points are drawn as outliers if they are smaller than $Q1-1.5*(Q3-Q1)$ or larger than $Q3+1.5*(Q3-Q1)$, where Q1 and Q3 are the 25th and 75th percentiles respectively. Young adult animals shown in blue, older adult animals shown in red. N = total number of either synchronised (a, value in a also applies to b) or mixed (c) response type recorded across animals.

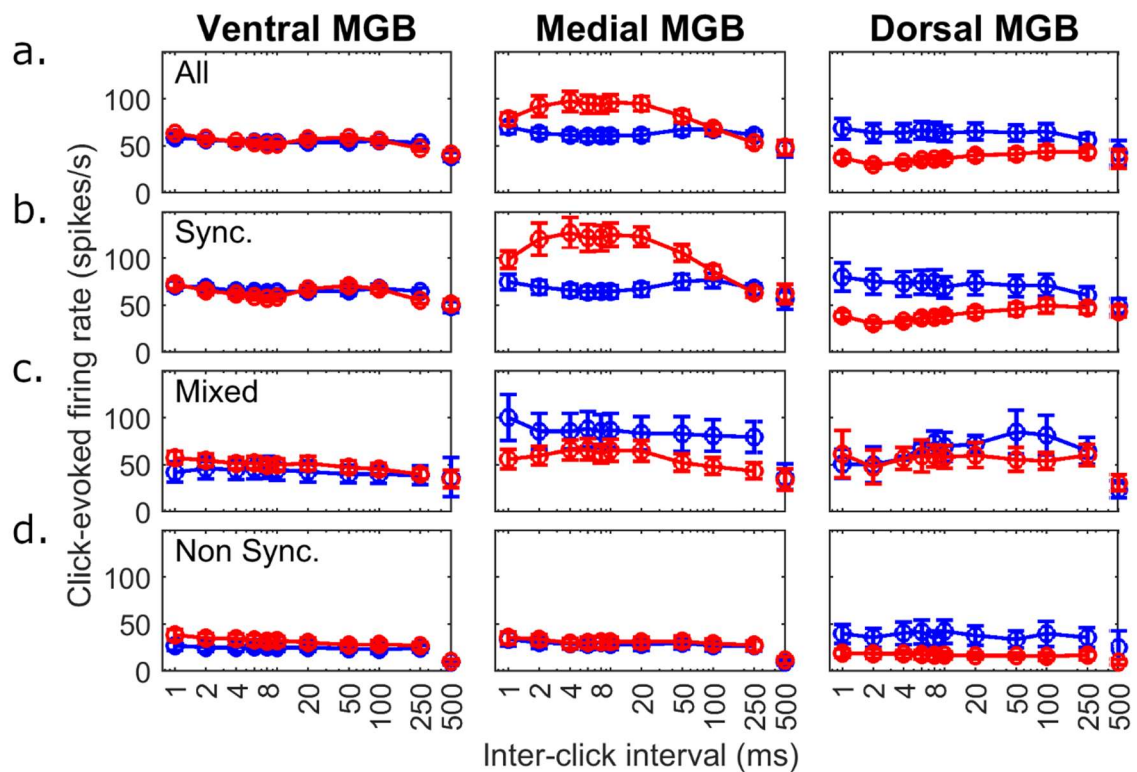


Figure 4. Ageing has a differential effect on firing rate which is dependent upon subdivision and response type. MGV neurons showed no age-related difference in firing rate regardless of the neural response pattern to click trains (a-d, left column), however, ageing leads to a click-rate dependent increase in mean firing rate of neurons recorded from MGM (a, middle column). This increase is only observed in synchronised MGM neurons (b, middle column) and for a limited range of ICIs. Older MGM neurons showing the mixed (c, middle column) or non-synchronised response type (d, middle column) do not show a significant difference in firing rate). Firing rates across all MGD were not significantly different between young and older adults, for any of the click rates tested (a, right column).

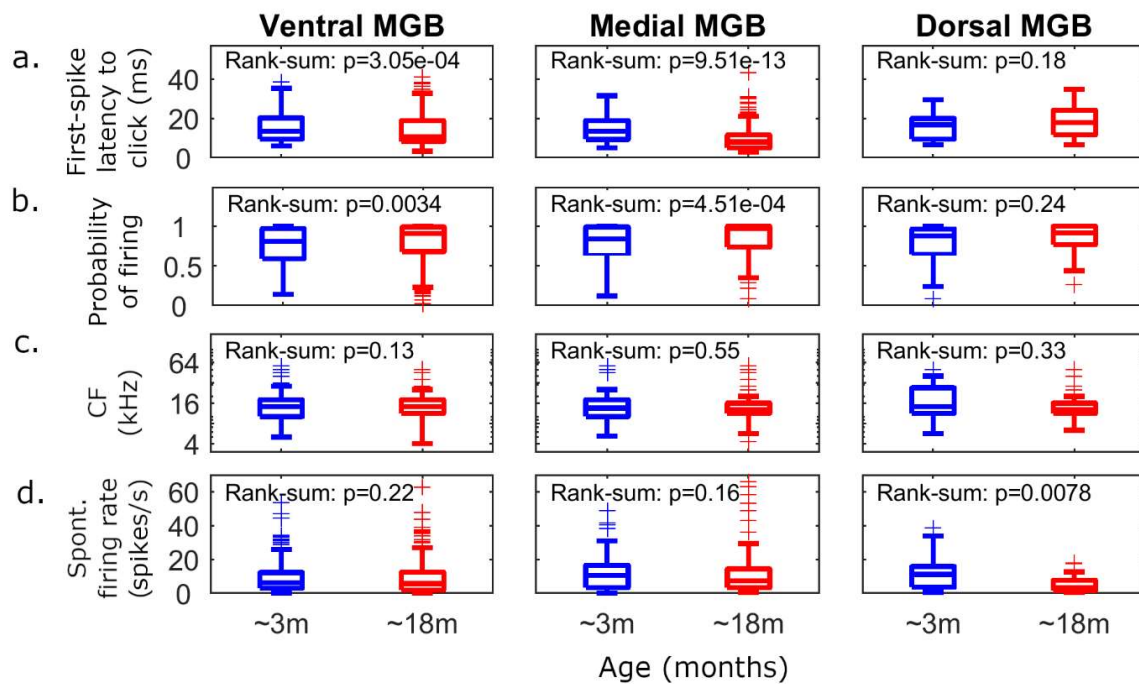


Figure 5. Ageing decreases first-spike latency and increases probability of firing in ventral and medial MGB (a&b, left and middle plots respectively), while responses in dorsal MGB remain unchanged (a&b, right). Ageing has no effect on characteristic frequency distribution across the MGB subdivisions (c), but spontaneous rates are observed to decrease in dorsal MGB (d, right). Young adult data shown in blue, older adult in red. Boxplot conventions as in Figure 3.

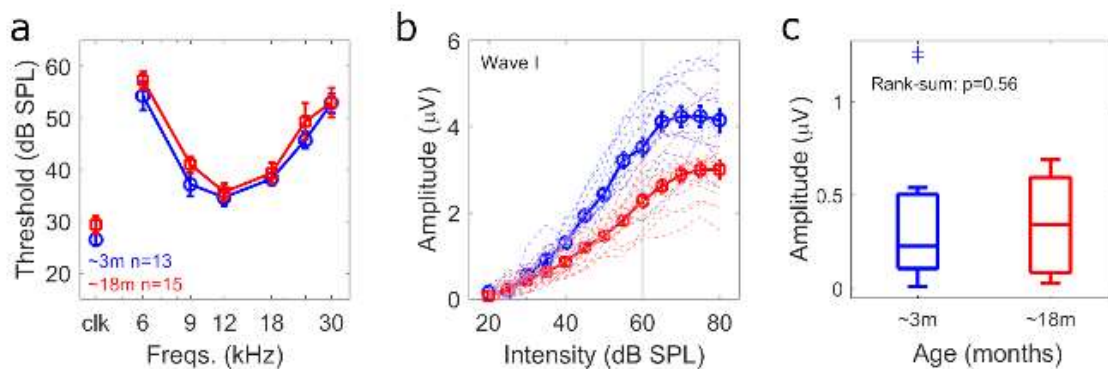
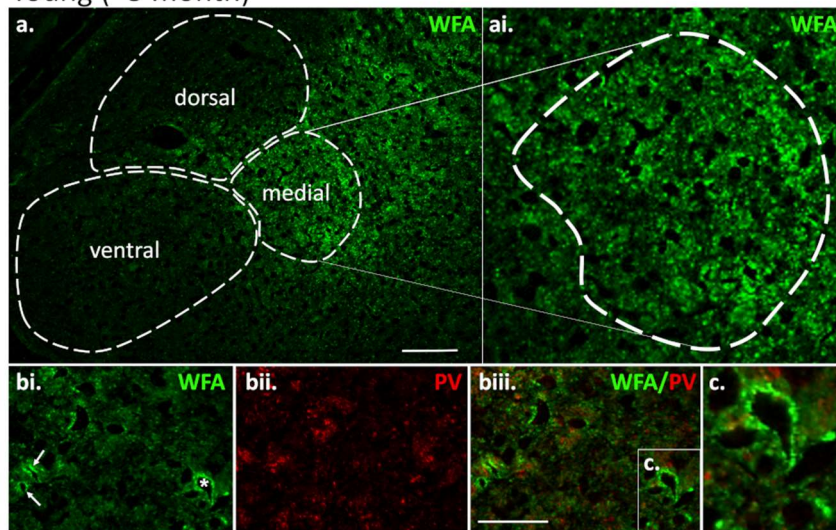
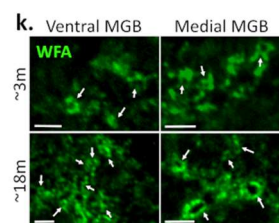
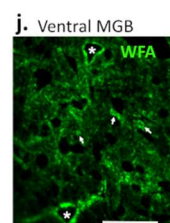
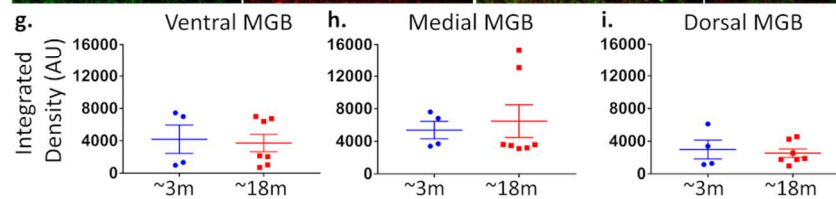
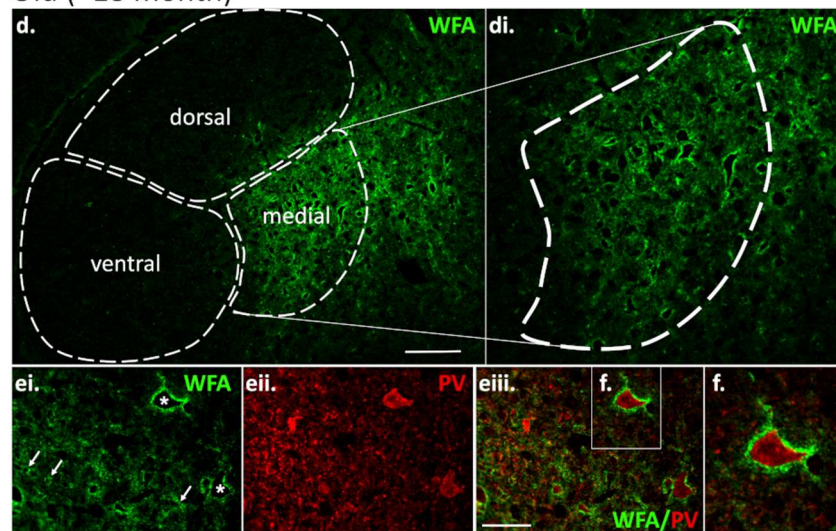


Figure 6. No difference in tone or click-evoked ABR thresholds for young and older adult CBA/Ca mice. A, audiogram shows no significant difference between young (blue) and older (red) adult CBA/Ca mice for click (clk) or tone stimuli at any of the frequencies tested. B, click-evoked growth functions of Wave I show no differences around threshold, but do show age-related decrease in amplitude of response with increasing sound intensity. Symbols and error-bars in a&b indicate mean \pm S.E.M. across animals, dashed lines in b show individual Wave I growth functions, grey line at 60 dB SPL highlights the sound level used to record thalamic responses to click trains. C, amplitude at threshold was not significantly different between young and older adult CBA/Ca mice. Boxplot conventions as per Figure 3.

Young (~3 month)



Old (~18 month)



MGB subdivision	PNN		Axonal Coats	
	~3m	~18m	~3m	~18m
Ventral	-	mod	v.low	low
Medial	mod	v.high	mod	v.high
Dorsal	-	v.low	v.low	v.low

Figure 7: MGB sub-division specific expression of PNNs and axonal coats. In young (a) and older (d) animals, WFA-fluorescence labelling of extracellular matrix components (green) was preferentially localised to MGM in comparison to MGCV or MGD. Diffuse extracellular matrix staining was observed in the MGB of young animals (a) with a modest number of condensed PNN structures surrounding neuronal cell bodies in MGM (a-c). In older animals, many PNN positive neurons labelled with WFA were observed in the MGM (d-f). WFA positive PNNs (asterisk) were also observed in the older MGCV

(j). PV expression (red) co-localised to some PNN+ neurons (asterisk) (e-f). However, PV-, PNN+ neurons (asterisks) were also observed (b-c). The fluorescent intensity of WFA in the MGB subdivisions did not show a statistically significant difference between young (blue: n=4) and older (red: n=7) animals (g-i). Each data point represents the average fluorescence intensity quantification from up to 2 slices per animal. Axonal coats (arrows) were present predominantly in MGM (b, e & k), with some WFA positive axonal coats (arrows) in MGv (j & k). PNN and axonal coats increased in the older animals compared to young in the MGB, as assessed by strength of expression and number of structures labelled by WFA (l). PNNs were defined by WFA immunostaining of the neuronal cell body/proximal dendrites, and axonal coats by size (2-5 μ M) and shape (round/oval). The MGM showed the greatest increase in PNNs and axonal coats in older animals (l). Mean \pm S.E.M., t-test MGv $p = 0.82$, MGM $p = 0.71$, MGD $p = 0.69$. Scale bars a & d: 100 μ M, b,iii, e,iii & j: 50 μ M, k: 10 μ M.

References

- Anderson, L.A., Izquierdo, M.A., Antunes, F.M., Malmierca, M.S., 2009. A monosynaptic pathway from dorsal cochlear nucleus to auditory cortex in rat. *Neuroreport* 20, 462–466. <https://doi.org/10.1097/WNR.0b013e328326f5ab>
- Anderson, L.A., Linden, J.F., 2016. Mind the Gap: Two Dissociable Mechanisms of Temporal Processing in the Auditory System. *J. Neurosci. Off. J. Soc. Neurosci.* 36, 1977–1995. <https://doi.org/10.1523/JNEUROSCI.1652-15.2016>
- Anderson, L.A., Linden, J.F., 2011. Physiological differences between histologically defined subdivisions in the mouse auditory thalamus. *Hear. Res.* 274, 48–60. <https://doi.org/10.1016/j.heares.2010.12.016>
- Anderson, L.A., Malmierca, M.S., Wallace, M.N., Palmer, A.R., 2006. Evidence for a direct, short latency projection from the dorsal cochlear nucleus to the auditory thalamus in the guinea pig. *Eur. J. Neurosci.* 24, 491–498. <https://doi.org/10.1111/j.1460-9568.2006.04930.x>
- Anderson, L.A., Shackleton, T.M., Palmer, A.R., 2005. Responses to amplitude-modulation in inferior colliculus and thalamus. Presented at the Association for Research in Otolaryngology, New Orleans, Louisiana, p. Abs.: 974.
- Anderson, S., Parbery-Clark, A., White-Schwoch, T., Dreihobl, S., Kraus, N., 2013. Effects of hearing loss on the subcortical representation of speech cues. *J. Acoust. Soc. Am.* 133, 3030–3038. <https://doi.org/10.1121/1.4799804>
- Bakay, W.M.H., Anderson, L.A., Garcia-Lazaro, J.A., McAlpine, D., Schaette, R., 2018. Hidden hearing loss selectively impairs neural adaptation to loud sound environments. *Nat. Commun.* 9, 4298. <https://doi.org/10.1038/s41467-018-06777-y>
- Balmer, T.S., 2016. Perineuronal Nets Enhance the Excitability of Fast-Spiking Neurons. *eNeuro* 3. <https://doi.org/10.1523/ENEURO.0112-16.2016>
- Banerjee, S.B., Gutzeit, V.A., Baman, J., Aoued, H.S., Doshi, N.K., Liu, R.C., Ressler, K.J., 2017. Perineuronal Nets in the Adult Sensory Cortex Are Necessary for Fear Learning. *Neuron* 95, 169–179.e3. <https://doi.org/10.1016/j.neuron.2017.06.007>

- Bartlett, E.L., Wang, X., 2011. Correlation of neural response properties with auditory thalamus subdivisions in the awake marmoset. *J. Neurophysiol.* 105, 2647–2667. <https://doi.org/10.1152/jn.00238.2010>
- Bartlett, E.L., Wang, X., 2007. Neural representations of temporally modulated signals in the auditory thalamus of awake primates. *J. Neurophysiol.* 97, 1005–1017. <https://doi.org/10.1152/jn.00593.2006>
- Beebe, N.L., Schofield, B.R., 2018. Perineuronal nets in subcortical auditory nuclei of four rodent species with differing hearing ranges. *J. Comp. Neurol.* 526, 972–989. <https://doi.org/10.1002/cne.24383>
- Bidelman, G.M., Villafuerte, J.W., Moreno, S., Alain, C., 2014. Age-related changes in the subcortical-cortical encoding and categorical perception of speech. *Neurobiol. Aging* 35, 2526–2540. <https://doi.org/10.1016/j.neurobiolaging.2014.05.006>
- Blosa, M., Sonntag, M., Jäger, C., Weigel, S., Seeger, J., Frischknecht, R., Seidenbecher, C.I., Matthews, R.T., Arendt, T., RübSamen, R., Morawski, M., 2015. The extracellular matrix molecule brevican is an integral component of the machinery mediating fast synaptic transmission at the calyx of Held. *J. Physiol.* 593, 4341–4360. <https://doi.org/10.1113/JP270849>
- Bozzelli, P.L., Alaiyed, S., Kim, E., Villapol, S., Conant, K., 2018. Proteolytic Remodeling of Perineuronal Nets: Effects on Synaptic Plasticity and Neuronal Population Dynamics. *Neural Plast.* 2018, 5735789. <https://doi.org/10.1155/2018/5735789>
- Brewton, D.H., Kokash, J., Jimenez, O., Pena, E.R., Razak, K.A., 2016. Age-Related Deterioration of Perineuronal Nets in the Primary Auditory Cortex of Mice. *Front. Aging Neurosci.* 8, 270. <https://doi.org/10.3389/fnagi.2016.00270>
- Bukalo, O., Schachner, M., Dityatev, A., 2007. Hippocampal metaplasticity induced by deficiency in the extracellular matrix glycoprotein tenascin-R. *J. Neurosci. Off. J. Soc. Neurosci.* 27, 6019–6028. <https://doi.org/10.1523/JNEUROSCI.1022-07.2007>
- Bukalo, O., Schachner, M., Dityatev, A., 2001. Modification of extracellular matrix by enzymatic removal of chondroitin sulfate and by lack of tenascin-R differentially affects several forms of synaptic plasticity in the hippocampus. *Neuroscience* 104, 359–369. [https://doi.org/10.1016/s0306-4522\(01\)00082-3](https://doi.org/10.1016/s0306-4522(01)00082-3)
- Burianova, J., Ouda, L., Profant, O., Syka, J., 2009. Age-related changes in GAD levels in the central auditory system of the rat. *Exp. Gerontol.* 44, 161–169. <https://doi.org/10.1016/j.exger.2008.09.012>
- Cai, R., Montgomery, S.C., Graves, K.A., Caspary, D.M., Cox, B.C., 2018. The FBN rat model of aging: investigation of ABR waveforms and ribbon synapse changes. *Neurobiol. Aging* 62, 53–63. <https://doi.org/10.1016/j.neurobiolaging.2017.09.034>
- Calford, M.B., Aitkin, L.M., 1983. Ascending projections to the medial geniculate body of the cat: evidence for multiple, parallel auditory pathways through thalamus. *J. Neurosci. Off. J. Soc. Neurosci.* 3, 2365–2380.
- Carstens, K.E., Dudek, S.M., 2019. Regulation of synaptic plasticity in hippocampal area CA2. *Curr. Opin. Neurobiol.* 54, 194–199. <https://doi.org/10.1016/j.conb.2018.07.008>
- Caspary, D.M., Hughes, L.F., Schatteman, T.A., Turner, J.G., 2006. Age-related changes in the response properties of cartwheel cells in rat dorsal cochlear nucleus. *Hear. Res.* 216–217, 207–215. <https://doi.org/10.1016/j.heares.2006.03.005>

- Caspary, D.M., Ling, L., Turner, J.G., Hughes, L.F., 2008. Inhibitory neurotransmission, plasticity and aging in the mammalian central auditory system. *J. Exp. Biol.* 211, 1781–1791. <https://doi.org/10.1242/jeb.013581>
- Caspary, D.M., Schatteman, T.A., Hughes, L.F., 2005. Age-related changes in the inhibitory response properties of dorsal cochlear nucleus output neurons: role of inhibitory inputs. *J. Neurosci. Off. J. Soc. Neurosci.* 25, 10952–10959. <https://doi.org/10.1523/JNEUROSCI.2451-05.2005>
- Chambers, A.R., Resnik, J., Yuan, Y., Whitton, J.P., Edge, A.S., Liberman, M.C., Polley, D.B., 2016a. Central Gain Restores Auditory Processing following Near-Complete Cochlear Denervation. *Neuron* 89, 867–879. <https://doi.org/10.1016/j.neuron.2015.12.041>
- Chambers, A.R., Salazar, J.J., Polley, D.B., 2016b. Persistent Thalamic Sound Processing Despite Profound Cochlear Denervation. *Front. Neural Circuits* 10, 72. <https://doi.org/10.3389/fncir.2016.00072>
- Cicanic, M., Edamatsu, M., Bekku, Y., Vorisek, I., Oohashi, T., Vargova, L., 2018. A deficiency of the link protein Bral2 affects the size of the extracellular space in the thalamus of aged mice. *J. Neurosci. Res.* 96, 313–327. <https://doi.org/10.1002/jnr.24136>
- Cisneros-Franco, J.M., Ouellet, L., Kamal, B., de Villers-Sidani, E., 2018. A Brain without Brakes: Reduced Inhibition Is Associated with Enhanced but Dysregulated Plasticity in the Aged Rat Auditory Cortex. *eNeuro* 5. <https://doi.org/10.1523/ENEURO.0051-18.2018>
- Edamatsu, M., Miyano, R., Fujikawa, A., Fujii, F., Hori, T., Sakaba, T., Oohashi, T., 2018. Hapln4/Bral2 is a selective regulator for formation and transmission of GABAergic synapses between Purkinje and deep cerebellar nuclei neurons. *J. Neurochem.* 147, 748–763. <https://doi.org/10.1111/jnc.14571>
- Fader, S.M., Imaizumi, K., Yanagawa, Y., Lee, C.C., 2016. Wisteria Floribunda Agglutinin-Labeled Perineuronal Nets in the Mouse Inferior Colliculus, Thalamic Reticular Nucleus and Auditory Cortex. *Brain Sci.* 6. <https://doi.org/10.3390/brainsci6020013>
- Favuzzi, E., Marques-Smith, A., Deogracias, R., Winterflood, C.M., Sánchez-Aguilera, A., Mantoan, L., Maeso, P., Fernandes, C., Ewers, H., Rico, B., 2017. Activity-Dependent Gating of Parvalbumin Interneuron Function by the Perineuronal Net Protein Brevican. *Neuron* 95, 639–655.e10. <https://doi.org/10.1016/j.neuron.2017.06.028>
- Fitzgibbons, P.J., Gordon-Salant, S., 1996. Auditory temporal processing in elderly listeners. *J. Am. Acad. Audiol.* 7, 183–189.
- Friauf, E., 2000. Development of chondroitin sulfate proteoglycans in the central auditory system of rats correlates with acquisition of mature properties. *Audiol. Neurootol.* 5, 251–262. <https://doi.org/10.1159/000013889>
- Frisina, D.R., Frisina, R.D., 1997. Speech recognition in noise and presbycusis: relations to possible neural mechanisms. *Hear. Res.* 106, 95–104.
- Gáti, G., Morawski, M., Lendvai, D., Jäger, C., Négyessy, L., Arendt, T., Alpár, A., 2010. Distribution and classification of aggrecan-based extracellular matrix in the thalamus of the rat. *J. Neurosci. Res.* 88, 3257–3266. <https://doi.org/10.1002/jnr.22493>
- Gordon-Salant, S., Fitzgibbons, P.J., Yeni-Komshian, G.H., 2011. Auditory Temporal Processing and Aging: Implications for Speech Understanding of Older People. *Audiol. Res.* 1. <https://doi.org/10.4081/audiore.2011.e4>

- Gray, D.T., Engle, J.R., Rudolph, M.L., Recanzone, G.H., 2014. Regional and age-related differences in GAD67 expression of parvalbumin- and calbindin-expressing neurons in the rhesus macaque auditory midbrain and brainstem. *J. Comp. Neurol.* 522, 4074–4084. <https://doi.org/10.1002/cne.23659>
- Guimaraes, P., Zhu, X., Cannon, T., Kim, S., Frisina, R.D., 2004. Sex differences in distortion product otoacoustic emissions as a function of age in CBA mice. *Hear. Res.* 192, 83–89. <https://doi.org/10.1016/j.heares.2004.01.013>
- Happel, M.F.K., Niekisch, H., Castiblanco Rivera, L.L., Ohl, F.W., Deliano, M., Frischknecht, R., 2014. Enhanced cognitive flexibility in reversal learning induced by removal of the extracellular matrix in auditory cortex. *Proc. Natl. Acad. Sci. U. S. A.* 111, 2800–2805. <https://doi.org/10.1073/pnas.1310272111>
- Heil, P., 2001. Representation of Sound Onsets in the Auditory System. *Audiol. Neurotol.* 6, 167–172. <https://doi.org/10.1159/000046826>
- Henry, K.R., 2004. Males lose hearing earlier in mouse models of late-onset age-related hearing loss; females lose hearing earlier in mouse models of early-onset hearing loss. *Hear. Res.* 190, 141–148. [https://doi.org/10.1016/S0378-5955\(03\)00401-5](https://doi.org/10.1016/S0378-5955(03)00401-5)
- Herrmann, B., Parthasarathy, A., Bartlett, E.L., 2017. Ageing affects dual encoding of periodicity and envelope shape in rat inferior colliculus neurons. *Eur. J. Neurosci.* 45, 299–311. <https://doi.org/10.1111/ejn.13463>
- Hirono, M., Watanabe, S., Karube, F., Fujiyama, F., Kawahara, S., Nagao, S., Yanagawa, Y., Misonou, H., 2018. Perineuronal Nets in the Deep Cerebellar Nuclei Regulate GABAergic Transmission and Delay Eyeblink Conditioning. *J. Neurosci. Off. J. Soc. Neurosci.* 38, 6130–6144. <https://doi.org/10.1523/JNEUROSCI.3238-17.2018>
- Huang, C.-Y., Winer, J.A., 2000. Auditory thalamocortical projections in the cat: laminar and areal patterns of input. *J. Comp. Neurol.* 427, 302–331. [https://doi.org/10.1002/1096-9861\(20001113\)427:2<302::aid-cne10>3.0.co;2-j](https://doi.org/10.1002/1096-9861(20001113)427:2<302::aid-cne10>3.0.co;2-j)
- Hughes, L.F., Turner, J.G., Parrish, J.L., Caspary, D.M., 2010. Processing of broadband stimuli across A1 layers in young and aged rats. *Hear. Res.* 264, 79–85. <https://doi.org/10.1016/j.heares.2009.09.005>
- Humes, L.E., Christopherson, L., 1991. Speech identification difficulties of hearing-impaired elderly persons: the contributions of auditory processing deficits. *J. Speech Hear. Res.* 34, 686–693.
- Humes, L.E., Roberts, L., 1990. Speech-recognition difficulties of the hearing-impaired elderly: the contributions of audibility. *J. Speech Hear. Res.* 33, 726–735.
- Hunter, K.P., Willott, J.F., 1987. Aging and the auditory brainstem response in mice with severe or minimal presbycusis. *Hear. Res.* 30, 207–218.
- Kajimura, J., Ito, R., Manley, N.R., Hale, L.P., 2016. Optimization of Single- and Dual-Color Immunofluorescence Protocols for Formalin-Fixed, Paraffin-Embedded Archival Tissues. *J. Histochem. Cytochem. Off. J. Histochem. Soc.* 64, 112–124. <https://doi.org/10.1369/0022155415610792>
- Kommajosyula, S.P., Cai, R., Bartlett, E., Caspary, D.M., 2019. Top-down or bottom up: decreased stimulus salience increases responses to predictable stimuli of auditory thalamic neurons. *J. Physiol.* 597, 2767–2784. <https://doi.org/10.1113/JP277450>

- Kotak, V.C., Fujisawa, S., Lee, F.A., Karthikeyan, O., Aoki, C., Sanes, D.H., 2005. Hearing Loss Raises Excitability in the Auditory Cortex. *J. Neurosci. Off. J. Soc. Neurosci.* 25, 3908–3918. <https://doi.org/10.1523/JNEUROSCI.5169-04.2005>
- Martin, J.S., Jerger, J.F., 2005. Some effects of aging on central auditory processing. *J. Rehabil. Res. Dev.* 42, 25–44.
- Matthews, R.T., Kelly, G.M., Zerillo, C.A., Gray, G., Tiemeyer, M., Hockfield, S., 2002. Aggrecan glycoforms contribute to the molecular heterogeneity of perineuronal nets. *J. Neurosci. Off. J. Soc. Neurosci.* 22, 7536–7547.
- Mendelson, J.R., Ricketts, C., 2001. Age-related temporal processing speed deterioration in auditory cortex. *Hear. Res.* 158, 84–94.
- Merabet, L.B., Pascual-Leone, A., 2010. Neural Reorganization Following Sensory Loss: The Opportunity Of Change. *Nat. Rev. Neurosci.* 11, 44–52. <https://doi.org/10.1038/nrn2758>
- Morikawa, S., Ikegaya, Y., Narita, M., Tamura, H., 2017. Activation of perineuronal net-expressing excitatory neurons during associative memory encoding and retrieval. *Sci. Rep.* 7, 46024. <https://doi.org/10.1038/srep46024>
- Mossop, J.E., Wilson, M.J., Caspary, D.M., Moore, D.R., 2000. Down-regulation of inhibition following unilateral deafening. *Hear. Res.* 147, 183–187. [https://doi.org/10.1016/S0378-5955\(00\)00054-X](https://doi.org/10.1016/S0378-5955(00)00054-X)
- Myers, A.K., Ray, J., Kulesza, R.J., 2012. Neonatal conductive hearing loss disrupts the development of the Cat-315 epitope on perineuronal nets in the rat superior olivary complex. *Brain Res.* 1465, 34–47. <https://doi.org/10.1016/j.brainres.2012.05.024>
- Occelli, F., Hasselmann, F., Bourien, J., Eybalin, M., Puel, J.L., Desvignes, N., Wiszniowski, B., Edeline, J.-M., Gourévitch, B., 2019. Age-related Changes in Auditory Cortex Without Detectable Peripheral Alterations: A Multi-level Study in Sprague–Dawley Rats. *Neuroscience* 404, 184–204. <https://doi.org/10.1016/j.neuroscience.2019.02.002>
- Ohlemiller, K.K., Dahl, A.R., Gagnon, P.M., 2010. Divergent Aging Characteristics in CBA/J and CBA/CAJ Mouse Cochleae. *JARO J. Assoc. Res. Otolaryngol.* 11, 605–623. <https://doi.org/10.1007/s10162-010-0228-1>
- Ouda, L., Profant, O., Syka, J., 2015. Age-related changes in the central auditory system. *Cell Tissue Res.* 361, 337–358. <https://doi.org/10.1007/s00441-014-2107-2>
- Pal, I., Paltati, C.R.B., Kaur, C., Shubhi Saini, null, Kumar, P., Jacob, T.G., Bhardwaj, D.N., Roy, T.S., 2019. Morphological and neurochemical changes in GABAergic neurons of the aging human inferior colliculus. *Hear. Res.* <https://doi.org/10.1016/j.heares.2019.02.005>
- Parthasarathy, A., Bartlett, E.L., 2011. Age-related auditory deficits in temporal processing in F-344 rats. *Neuroscience* 192, 619–630. <https://doi.org/10.1016/j.neuroscience.2011.06.042>
- Peelle, J.E., Troiani, V., Wingfield, A., Grossman, M., 2010. Neural processing during older adults' comprehension of spoken sentences: age differences in resource allocation and connectivity. *Cereb. Cortex N. Y. N* 1991 20, 773–782. <https://doi.org/10.1093/cercor/bhp142>
- Presacco, A., Simon, J.Z., Anderson, S., 2019. Speech-in-noise representation in the aging midbrain and cortex: Effects of hearing loss. *PLoS One* 14, e0213899. <https://doi.org/10.1371/journal.pone.0213899>

- Presacco, A., Simon, J.Z., Anderson, S., 2016a. Effect of informational content of noise on speech representation in the aging midbrain and cortex. *J. Neurophysiol.* 116, 2356–2367. <https://doi.org/10.1152/jn.00373.2016>
- Presacco, A., Simon, J.Z., Anderson, S., 2016b. Evidence of degraded representation of speech in noise, in the aging midbrain and cortex. *J. Neurophysiol.* 116, 2346–2355. <https://doi.org/10.1152/jn.00372.2016>
- Recanzone, G., 2018. The effects of aging on auditory cortical function. *Hear. Res.* 366, 99–105. <https://doi.org/10.1016/j.heares.2018.05.013>
- Richardson, B.D., Ling, L.L., Uteshev, V.V., Caspary, D.M., 2013. Reduced GABA(A) receptor-mediated tonic inhibition in aged rat auditory thalamus. *J. Neurosci. Off. J. Soc. Neurosci.* 33, 1218–1227a. <https://doi.org/10.1523/JNEUROSCI.3277-12.2013>
- Romberg, C., Yang, S., Melani, R., Andrews, M.R., Horner, A.E., Spillantini, M.G., Bussey, T.J., Fawcett, J.W., Pizzorusso, T., Saksida, L.M., 2013. Depletion of perineuronal nets enhances recognition memory and long-term depression in the perirhinal cortex. *J. Neurosci. Off. J. Soc. Neurosci.* 33, 7057–7065. <https://doi.org/10.1523/JNEUROSCI.6267-11.2013>
- Rouiller, E., de Ribaupierre, Y., Toros-Morel, A., de Ribaupierre, F., 1981. Neural coding of repetitive clicks in the medial geniculate body of cat. *Hear. Res.* 5, 81–100.
- Rouiller, E.M., 1997. Functional organisation of the auditory pathways, in: Ehret, G., Romand, R. (Eds.), *The Central Auditory System*. Oxford University Press.
- Rouiller, E.M., de Ribaupierre, F., 1985. Origin of afferents to physiologically defined regions of the medial geniculate body of the cat: ventral and dorsal divisions. *Hear. Res.* 19, 97–114.
- Rowlands, D., Lensjø, K.K., Dinh, T., Yang, S., Andrews, M.R., Hafting, T., Fyhn, M., Fawcett, J.W., Dick, G., 2018. Aggrecan Directs Extracellular Matrix-Mediated Neuronal Plasticity. *J. Neurosci. Off. J. Soc. Neurosci.* 38, 10102–10113. <https://doi.org/10.1523/JNEUROSCI.1122-18.2018>
- Schatteman, T.A., Hughes, L.F., Caspary, D.M., 2008. Aged-Related Loss of Temporal Processing: Altered Responses to Amplitude Modulated Tones in Rat Dorsal Cochlear Nucleus. *Neuroscience* 154, 329–337. <https://doi.org/10.1016/j.neuroscience.2008.02.025>
- Schnell, S.A., Staines, W.A., Wessendorf, M.W., 1999. Reduction of lipofuscin-like autofluorescence in fluorescently labeled tissue. *J. Histochem. Cytochem. Off. J. Histochem. Soc.* 47, 719–730. <https://doi.org/10.1177/002215549904700601>
- Schofield, B.R., Motts, S.D., Mellott, J.G., Foster, N.L., 2014. Projections from the dorsal and ventral cochlear nuclei to the medial geniculate body. *Front. Neuroanat.* 8, 10. <https://doi.org/10.3389/fnana.2014.00010>
- Scholl, B., Wehr, M., 2008. Disruption of Balanced Cortical Excitation and Inhibition by Acoustic Trauma. *J. Neurophysiol.* 100, 646–656. <https://doi.org/10.1152/jn.90406.2008>
- Sergeyenko, Y., Lall, K., Liberman, M.C., Kujawa, S.G., 2013. Age-related cochlear synaptopathy: an early-onset contributor to auditory functional decline. *J. Neurosci. Off. J. Soc. Neurosci.* 33, 13686–13694. <https://doi.org/10.1523/JNEUROSCI.1783-13.2013>
- Sonntag, M., Blosa, M., Schmidt, S., Rübsamen, R., Morawski, M., 2015. Perineuronal nets in the auditory system. *Hear. Res.* 329, 21–32. <https://doi.org/10.1016/j.heares.2014.12.012>

- Sottile, S.Y., Hackett, T.A., Cai, R., Ling, L., Llano, D.A., Caspary, D.M., 2017. Presynaptic Neuronal Nicotinic Receptors Differentially Shape Select Inputs to Auditory Thalamus and Are Negatively Impacted by Aging. *J. Neurosci. Off. J. Soc. Neurosci.* 37, 11377–11389. <https://doi.org/10.1523/JNEUROSCI.1795-17.2017>
- Spongr, V.P., Flood, D.G., Frisina, R.D., Salvi, R.J., 1997. Quantitative measures of hair cell loss in CBA and C57BL/6 mice throughout their life spans. *J. Acoust. Soc. Am.* 101, 3546–3553. <https://doi.org/10.1121/1.418315>
- Stebbing, K.A., Choi, H.W., Ravindra, A., Caspary, D.M., Turner, J.G., Llano, D.A., 2016. Ageing-related changes in GABAergic inhibition in mouse auditory cortex, measured using in vitro flavoprotein autofluorescence imaging. *J. Physiol.* 594, 207–221. <https://doi.org/10.1113/JP271221>
- Tremblay, M.-È., Zettel, M.L., Ison, J.R., Allen, P.D., Majewska, A.K., 2012. Effects of aging and sensory loss on glial cells in mouse visual and auditory cortices. *Glia* 60, 541–558. <https://doi.org/10.1002/glia.22287>
- Ueno, H., Fujii, K., Takao, K., Suemitsu, S., Murakami, S., Kitamura, N., Wani, K., Matsumoto, Y., Okamoto, M., Ishihara, T., 2019. Alteration of parvalbumin expression and perineuronal nets formation in the cerebral cortex of aged mice. *Mol. Cell. Neurosci.* 95, 31–42. <https://doi.org/10.1016/j.mcn.2018.12.008>
- van 't Spijker, H.M., Kwok, J.C.F., 2017. A Sweet Talk: The Molecular Systems of Perineuronal Nets in Controlling Neuronal Communication. *Front. Integr. Neurosci.* 11, 33. <https://doi.org/10.3389/fnint.2017.00033>
- Walton, J.P., Frisina, R.D., O'Neill, W.E., 1998. Age-related alteration in processing of temporal sound features in the auditory midbrain of the CBA mouse. *J. Neurosci. Off. J. Soc. Neurosci.* 18, 2764–2776.
- Wang, H., Brozoski, T.J., Caspary, D.M., 2011. Inhibitory neurotransmission in animal models of tinnitus: Maladaptive plasticity. *Hear. Res., Synaptic Plasticity* 279, 111–117. <https://doi.org/10.1016/j.heares.2011.04.004>
- Wegner, F., Härtig, W., Bringmann, A., Grosche, J., Wohlfarth, K., Zuschratter, W., Brückner, G., 2003. Diffuse perineuronal nets and modified pyramidal cells immunoreactive for glutamate and the GABA(A) receptor alpha1 subunit form a unique entity in rat cerebral cortex. *Exp. Neurol.* 184, 705–714. [https://doi.org/10.1016/S0014-4886\(03\)00313-3](https://doi.org/10.1016/S0014-4886(03)00313-3)
- Weinrich, L., Sonntag, M., Arendt, T., Morawski, M., 2018. Neuroanatomical characterization of perineuronal net components in the human cochlear nucleus and superior olivary complex. *Hear. Res.* 367, 32–47. <https://doi.org/10.1016/j.heares.2018.07.005>
- Willott, J.F., 1986. Effects of aging, hearing loss, and anatomical location on thresholds of inferior colliculus neurons in C57BL/6 and CBA mice. *J. Neurophysiol.* 56, 391–408. <https://doi.org/10.1152/jn.1986.56.2.391>
- Winer, J.A., 1992. The Functional Architecture of the Medial Geniculate Body and the Primary Auditory Cortex, in: Webster, D.B., Popper, A.N., Fay, R.R. (Eds.), *The Mammalian Auditory Pathway: Neuroanatomy*, Springer Handbook of Auditory Research. Springer New York, New York, NY, pp. 222–409. https://doi.org/10.1007/978-1-4612-4416-5_6

Zheng, Y., Escabí, M.A., 2013. Proportional spike-timing precision and firing reliability underlie efficient temporal processing of periodicity and envelope shape cues. *J. Neurophysiol.* 110, 587–606. <https://doi.org/10.1152/jn.01080.2010>